A NEW PENALTY STIFFNESS TREATMENT

FOR MASTER-SLAVE CONTACT SURFACES

A NEW PENALTY STIFFNESS TREATMENT FOR MASTER-SLAVE CONTACT SURFACES

By

Yihai Shi, B.Sc.

A Thesis

Submitted to the School of Graduate Studies

In Partial Fulfillment of the Requirements

For the Degree

Master of Engineering

McMaster University

September 2001

MASTER OF ENGINEERING
(Mechanical Engineering)

McMaster University

TILTE: A NEW PENALTY STIFFNESS TREATMENT FOR MASTER-SLAVE CONTACT SURFACES

AUTHOR: Yihai Shi B. Sc. (Mech. Eng.)
Shanghai University of Engineering

SUPERVISOR: Dr. Don Metzger, Associate Professor
Department of Mechanical
McMaster University

NUMBER OF PAGES: X, 101

ABSTRACT

Finite element simulation of contact/impact problems using the penalty method is a well-established capability. The automatic penalty stiffness provides an easy way to implement the contact analysis. However, this way in which the penalty stiffness is associated with the material property and geometry of the master surface can lead to inappropriate distributions of contact pressure at edges or mesh transitions, or even cause much numerical noise. A new method of defining the penalty stiffness, which is associated with geometry of the slave surface, the reference penetration and reference contact pressure, is developed to consistently relate forces on contacting nodes with the contact pressure. This technique is successfully applied to several examples as the clamping simulation during the punch test and the rolling process. The results of such applications of new contact stiffness model demonstrate the effectiveness of such a model in avoiding the stress edge effect and the accompanying numerical noise. As an alternative approach to define the penalty stiffness, this new model provides another option for the contact analysis and gives the users more possibilities to control the contact performance.

ACKNOWLEDGEMENTS

I would like to express my great appreciation to Dr. Don Metzger for his advice and encouragement during the creation of this thesis. Without his kindness and supervision, I can not imagine that this thesis could have been done effectively and timely. Also, thanks to my close friends Kim YoungSuk and Pan Li for their constructive advice in the completion of this work.

TABLE OF CONTENTS

LIST OF FIGURES

CHAPTER 1

INTRODUCTION

1.1 Introduction to the Contact Problem

Contact problems involve the interaction between two or more parts coming into contact with each other. Contact-impact phenomena are quite common in our lives: a typical example is the vehicle crash. In engineering, the contact interactions are usually intentional such as the metal forming process, in which the form of the part is achieved through the contact interaction of punch and metal sheet, die and metal sheet. Although contact phenomena are common in both life and engineering applications, the effects are often accounted for approximately due to complexity of the analysis. For many practical applications, the experiment may be an easy and economical way to get straight results, which can avoid complicated calculation. In some circumstances, the cost of the experiment makes it undesirable to use such tests as the car crash experiment, or if safety issues make such experiments impossible such as nuclear reactor components. Furthermore, the knowledge of the mechanism of the contact interaction will be desired since it can benefit us with its prediction of possible outcomes that can have practical usage. For example, the simulation of the machining process will lead to the better understanding of the stress buildup during the machining and such knowledge will directly improve the design of the tool by enhancing the quality of machining and life

span of the machine tool. Obviously, the understanding of the contacting mechanism will also lead to the better performance of the intentional contact practice and the avoidance of the unexpected contact behavior in engineering applications. All such motivations led to many people to simulate contact since the last century.

Studies of contact problems in the first stage came with Newton's third law and Coulomb's friction law which are still used in many analyses. Suppose two blocks (Fig. 1-1) come into contact with each other. The contact force and the frictional force are subjected to the following conditions:

$$F_1 = F_2, N_1 = N_2 \qquad \text{(Newton's third law)}$$

$$F_1 \le \mu_1 N_1 \qquad \text{(Coulomb's friction law)} \qquad \text{(1-1)}$$

$$F_3 \le \mu_2 N_3$$

where μ_1, μ_2 are the frictional coefficient between body A and body B, body B and ground. When the tangential force is less than the product of normal force and the friction coefficient, the bodies remain in the relative static state (sticking). If the tangential force exceeds such a value, the bodies will enter the state of sliding.

The major difficulty of this approach is that it can not determine the stress distribution along the contacting surface. Rather, the bodies are assumed rigid and only resultant forces are considered. In practical work, the contact stress on or beneath the contact surface may be more important since many material failures are due to the high

stress concentration at the specific contact area. Hertz did a significant study and developed a model to present such stress during the contact. The model, which assumes contact to be an elastic problem with small deformation, shows that pressure distribution along the contact surface is in a form of ellipse in a frictionless model. The maximum stress and shear stress (Fig.1-2) according to Hertz model [1] are as follows

$$\sigma_{max} = -c_\sigma C \qquad \tau_{max} = c_\tau C \tag{1-2}$$

where c_σ, c_τ are the normal and shear stress coefficients for the contact bodies which is determined by the contacting conditions and material properties.

Although Hertzian contact theory demonstrates the force distribution or the contacting stress on the contact surfaces, there are many restrictions:

1) The contact body must be linearly elastic.

2) There can be no friction force along the contact surfaces.

3) The displacement must be very small.

Such restrictions limit its application since many problems involving the friction, material nonlinear characteristics or large deformation (nonlinear geometry) are beyond the scope of such methods. Following the Hertz's work, research has been focused on the solution of the contact problem by the analytical and experimental approaches. Johnson [2] studied the contact with analytical methods to release some of the constraints on the Hertzian contact problems. During this stage, geometry and deformation of the contact

bodies are assumed in such a way that available mathematical tools can be used to get analytical (closed-form) solutions to contact/impact problems. Such methods are still too restrictive and limit their applications to special problems. The breakthrough of such research was brought by introducing the numerical technique with the development of the digital computer and finite element method, all of which bring the research of the contact problem to a higher level of complexity.

1.2 Finite Element Method to Solve the Contact Problem

The finite element method has been developed to solve the problems of continuum and structural deformation and loading which are so complicated in either geometry configuration or material consideration that the traditional analytical approach is unable to get a closed-form solution. Thus, a numerical technique must be applied to find accurate approximation. Contact/impact problems are such typical cases. The literature shows that finite element method solution of contact problems had been investigated for a long time and its method and application touch almost every aspect of engineering. Zhong [3] gave a detailed list of the problems solved by the finite element method for different contact problems. In metal cutting problems, Strenkowski [4] for the first time introduced the concept of the element deletion based on the effective plastic strain to simulate the contact interaction between the work piece and tool, and successfully analyzed the orthogonal metal cutting. Following this, Obikawa et al [5], Shih [6] and Black et al [7] developed new geometric mesh separation criteria and friction contact models to simulate the contact in machining process in the 3D model.

Rolling processes have also drawn attention: J. J. Park et al [8], Bhargava et al [9] and Kulkarni et al [10] presented a typical contact simulation for the plane-strain rolling and plate rolling in 3-D model. The regular mechanical engineering contact interaction has also been tried in applications such as bearings by Cheng et al [11] and Torstenfelt [12], the fitting of shafts to sleeve and hubs by Okamato et al [13] and Francisc [14].

In general, the basic ingredients for the finite element procedure to solve contact problems may be summarized as follows:

1. Variational formulation which provides a basis for the finite element discretization.

2. Element formulation which calculates the basis of finite element discretization for the continuum and create the matrix and load vector equations.

3. Material selection which determines the strain and stress relations for the element formulation.

4. Contact restraint method which applies the restraint conditions on the contact bodies.

5. Friction law which governs the friction force and motion between contact bodies

6. Contacting searching algorithm.

7. Numerical time integration method.

Due to specific characteristics of the contact, the finite element solution of contact problems has typical features. The following sections concern the main categories of the research on contact problems using the finite element method.

1.3 Contact Restraint

Contact and impact problems involve the contact restraints that must be imposed on the contact boundaries. Numerically, the constraint equations are introduced to the governing equations to enforce the impenetrability and sticking and sliding condition of the contact bodies. Typically, there are two basic methods: the penalty method and the Lagrange multiplier method. Both methods can be applied to the system via the principle of stationary potential energy. For a conservative mechanical system, the total potential energy will include strain energy of distorted bodies and the potential possessed by the applied loads. The potential energy of a discretized system [15], [16] can be expressed in the conventional finite element procedure as follows:

$$\Pi=\frac{1}{2}\{u\}^T K\{u\}-\{u\}^T F \tag{1-3}$$

where Π is the potential energy of the system, K is the stiffness of the system, $\{u\}$ is the displacement of the node vector and F is the external force applied on the specific nodes. The principle of stationary potential energy states that:

Among all admissible configuration of a conservation system, those that satisfy the equations of equilibrium make the potential stationary with respect to small admissible variations of displacement.

In the contact problem, the contacting restraints can be added to potential energy as a specific potential function in following two methods:

1.3.1 The Lagrange Multiplier Method

A concise mathematical consideration of contact constraints can be obtained with the use of a method called the Lagrange multiplier method [3], [15]. The Lagrange multiplier method introduces the contact constraint equation by use of extra unknowns, the Lagrange multipliers. These multipliers, upon solving the augmented system of equations, represent the reaction forces at constrained degrees of freedom.

During the contact, a gap function G representing constraint conditions is introduced to correspond with the initial distance between the two contacting bodies. The gap function decreases with the hitting body approaching the target body and becomes zero when both touch. The gap function is required to keep positive all the relative displacements during the contact, which is determined by the nature of the contact condition. That is:

$$G(u) \geq 0 \tag{1-4}$$

Gap function can be expressed as a function of displacement by using the Taylor series:

$$G(u) = G_0 + \frac{\partial G}{\partial u}\{u\} = G_0 + g\{u\} \tag{1-5}$$

where the higher order derivatives of the gap function are ignored and g is first order derivative of G with respect to u.

To enforce such constraint conditions to the equation (1-3), a free scale λ Lagrange multiplier is multiplied to the gap function and added to the potential functional.

$$\Pi(u,\lambda) = \frac{1}{2}\{u\}^T K\{u\} - \{u\}^T F + \lambda^T (G_0 + g\{u\}) \tag{1-6}$$

The principle of stationary potential energy is applied to the equation (1-6) to give

$$\frac{\partial \Pi}{\partial u} = K\{u\} - F + \lambda g^T = 0$$

$$\frac{\partial \Pi}{\partial \lambda} = g\{u\} + G_0 = 0 \tag{1-7}$$

Equation (1-7) in a matrix form is as follows:

$$\begin{bmatrix} K & g^T \\ g & 0 \end{bmatrix} \begin{Bmatrix} u \\ \lambda \end{Bmatrix} = \begin{bmatrix} F \\ -G_0 \end{bmatrix} \tag{1-8}$$

The lower partition of above equation is the equation of constraint and equation (1-8) is solved for both λ and $\{u\}$. The satisfaction of the equation (1-8) automatically imposes the contact constraints to the system. By solving the equations, the displacement $\{u\}$ and

Lagrange multiplier λ will be obtained. The Lagrange multiplier λ is interpreted as the contacting forces at corresponding contacting nodes. Examples for the application of Lagrange multiplier method in solving the contact problems are presented by Bathe [17] and Katona [18], in which it is coupled with the implicit methods giving an efficient way to obtain a solution.

An obvious disadvantage of the Lagrange multiplier method is that it introduces the new variable λ, which increases the bandwidth of the matrix of the whole contact system and correspondingly decreases the calculation efficiency of the solution. Such a disadvantage becomes more obvious for multi-body contact, which makes the Lagrange multiplier method inefficient for some contact analyses.

1.3.2 The Penalty Method

Another typical way to apply the contact constraints, the penalty method, can overcome such disadvantages and is widely used in the explicit method. To introduce the basic constraints in the penalty method [19], [20], a penalty function is applied to the contacting bodies according to a potential.

$$\pi_p = \frac{1}{2}\delta^T \alpha \delta \tag{1-9}$$

where α is penalty stiffness applied to approximately enforce the contact restraint on the contacting bodies, and δ is the penetration function (finite penetration allowed) when the

contact occurs between the contacting bodies. The forces associated with the penalty function are given by the product of the penetration and the penalty stiffness.

$$f_p = \alpha\delta \tag{1-10}$$

The penetration function can be written as a function of nodal displacement in terms of a Taylor series expansion with the higher order derivatives ignored:

$$\delta(u) = \delta_0 + \frac{\partial\delta}{\partial u}\{u\} = \delta_0 + Q\{u\} \tag{1-11}$$

In the equation (1-11), δ_0 is the penetration of each contacting node, and Q is a matrix of the partial derivatives of the penetration function for each contacting node.

Upon substitution of equation (1-11) into equation (1-9), the potential function to be minimized becomes

$$\begin{aligned}\Pi &= \frac{1}{2}\{u\}^T K\{u\} - \{u\}^T F + \frac{1}{2}\delta^T\alpha\delta \\ &= \frac{1}{2}\{u\}^T K\{u\} - \{u\}^T F + \frac{1}{2}(\delta_0 + Q\{u\})^T\alpha(\delta_0 + Q\{u\})\end{aligned} \tag{1-12}$$

After applying the principle of stationary potential energy to the equation (1-12), it takes the form:

$$\frac{\partial\Pi}{\partial u} = (K + Q^T\alpha Q)\{u\} - F + Q^T\alpha\delta_0 = 0 \tag{1-13}$$

Writen in a conventional finite element form, this is

$$(K + Q^T \alpha Q)\{u\} = F - Q^T \alpha \delta_0 \tag{1-14}$$

It is clear from the equation (1-14) that in the penalty method, the penalty function as a constraint function changes the stiffness of the system when the contact conditions have been activated. The penalty matrix may significantly increase the bandwidth of the structural equations which depends on how many degrees of freedom are introduced and numbered and what degrees of freedom are coupled by the constraint equations. Also, in the penalty method, the penalty stiffness must be chosen in an allowable range since the contact penalty stiffness will greatly influence the solution. The penalty stiffness must be large enough to be effective in keeping penetrations small but not as large as to provoke the numerical difficulties [21]. For example, if the penalty stiffness is too big, it will cause the ill conditioning of the system matrix and instability of the solution. Such an effect will be discussed in the following chapters.

The penalty method is extensively used in the finite element analysis of contact problems since it has a simple form of application and there are no new degrees of freedom introduced. Its simplicity is the big advantage over the Lagrange multiplier method. Kikuchi [22] presented a smoothing technique for oscillating contact pressure created by the penalty method. Chandrasekaran [23] successfully presented 2-D frictional contact model with the penalty method by imposing geometric constraints on the pseudo equilibrium configuration. Kulak [24] introduced an adaptive interface elements based on the penalty method to handle the changing contact configuration allowing for surface sliding. When the penalty method is coupled with the master-slave

(slide-line) approach in an explicit transient finite element method [25], [26], [27], it takes on a more closed and efficient form to solve the complex three-dimensional problems.

1.4 Contact Searching Approaches

In the finite element method for contact problems, another main topic is the contact searching approach, the purpose of which is to locate the hitting nodes to the potential targets. An effective searching algorithm normally influences the reliability and efficiency of the numerical solution and even determines the success of the final solution. Much effort has been made so far to find an effective way. For example, Hallquist [28] and Samual [29] presented the general concept and method to treat the sliding interface between the contact surfaces. In the specific application of searching algorithm for the contact problems, Manuel et al. [30] focused on the metal forming process, Belytschko [31] presented the pinball algorithm for both the penalty and Lagrangian multiplier method, and Jerry et al. [32] developed the 3-D impact-penetration algorithm with erosion. The typical contact searching approaches are discussed below.

1.4.1 Node-to-Node Contact Searching

In the node-to-node searching algorithm, it is assumed that contacting bodies can only undergo small displacement and rotation, and the contacting boundaries are discretized such that only the nodes on the boundaries can get into contact. This contact searching is used in the early study by Zienkiewicz [33] and Okamoto [13]. Since it

imposed many restrictions during the solution, the node-to-node contact searching is seldom used in the large deformation and complicated geometry problem.

1.4.2 Bucketing Searching

This method was developed by Hallquist [25] which allows the contact between the nodes and surfaces. In this algorithm, all contact surfaces are set as a single set of contact groups. The searching procedure is performed in three stages:

1) A target node which is closest to the hitting node is found.

2) The target segment containing the target node which is closest to the hitting node is found.

3) The distance between the hitting node and target segment is calculated, if the penetration is negative, the contact forces proportional to such penetration are applied to hitting node and nodes on the target segment.

During searching for closest target node to a specific hitting node, the bucketing searching (fig.1-3) is used, which defines a sorting of the nodes in relative buckets. To find the closest node for a given hitting node, it is only needed to compare the hitting node with those in the same bucket as the hitting node or within a neighboring bucket of the bucket containing the hitting node. The length size of bucket should be defined such that largest segment can be completely included in the buckets. If the given hitting node located in one specific bucket, its left and right neighboring buckets are to be selected in a comparison. The bucketing searching algorithm provides a general approach for the 3D contact

problem. The size of the bucket must be properly chosen to keep an efficient searching calculation, especially for a big model containing hundreds of thousands of nodes.

1.4.3 Master-Slave Searching

The master-slave searching approach is extensively used in most finite element codes such as LS-DYNA [25], ABAQUS [26] and H3DMAP [27] since it has simple form when coupled with the friction model. In the master-slave searching, the approaches of the searching steps are the same in the bucketing searching. But the contacting hitting surface and target surface have to be predefined as the slave and master surface before the process. To find the closest target node for a given hitting node, only the corresponding master surface which containing the target nodes will be examined. All the remaining surface elements are ignored during the searching procedure.

The master-slave searching approach is conceptually simple, but, since it needs to predefine the pair of the contacting surface, problems will become complicated and inefficient for the contact problems which involve the newly generated contact surfaces. Such an example is the machining problem, where the chip formation during the machining makes simulation complex by using the master-slave searching approach since contact restraints may not be practically specified by predefined contact sets. In such circumstances, either an additional searching algorithm to find the new contact sets, or specification of all potential contacts should be applied. Either way, computational efficiency can suffer greatly. Still the master-slave method is often highly successful, and a detailed discussion of master-slave searching approach is presented in the next chapter.

1.5 Friction in the Contact Problem

Friction phenomena exist in all contact problems, and in many engineering applications, the effects of the friction play an important role. For example, in the metal forming process, the friction between the work piece and the tool greatly influences the forming process and quality of the product. So far, much research has been done to solve contact problems with friction in the finite element method. Gu [34], Haber [35] and Hallquist [45] successfully simulated the sliding model between the contact surfaces. Sauve [27] solved the friction problem by using a non-classical friction law. N. Patir [36] used the hydrodynamic lubrication theory to simulate the lubrication and friction in the bulk metal-forming processes, followed by the K.K. Sun [37] and W. R. D. Wilson [38]. Also, W. K. Liu [39] applied the Arbitrary Lagrangian-Eulerian finite element elements along with the hydrodynamic lubrication finite element to simulate the friction force and lubricant flow during the metal forming process. This put the research of friction in FEA method into more practical situations. Typically, the conventional friction laws in contact problem model by using finite element method may be classified in the two ways described below.

1.5.1 Classical Friction Law

In the classical law of friction, there are two stages when contact occurs between bodies: sticking and sliding. If the two bodies are at rest or moving together without relative motion, the two bodies are supposed to be in a state of sticking, and friction force is calculated by multiplying the normal force perpendicular to the contact surface with the

static friction coefficient. If the tangential force exceeds this product, the dynamic coefficient of friction will be used to calculate the friction force as:

$$F_t = -\mu_d F_n \left(\frac{v_t}{|v_t|}\right) \tag{1-15}$$

where μ_d is the dynamical friction coefficient, v_t is the relative motion of the contacting bodies.

1.5.2 Non-Classic Laws of Friction

Non-classical law friction has been well presented by Fredriksson [40] to overcome the physical deficiency in the contact problem encountered when using the classical friction law. In engineering applications, the elastic-plasticity friction model is well established under numerical procedures in [25], [26], [27]. During contact, the relation between the frictional force f_t and tangential displacement u_t is plotted in Fig. 1-4, where a constant normal contact is assumed. When $|f_t|$ is smaller than the friction limit f_c, the relation between f_t and u_t is given by:

$$f_t = -E_f u_t \tag{1-16}$$

where E_f is the slope.

When the friction reaches the limit, the limiting value of tangential force is applied in the direction of tangential motion.

1.6 Contact Penalty Stiffness in the Penalty Method

As mentioned earlier, in the finite element method to solve contact problems, the penalty method has been extensively used with the explicit approach because it has a simple closed form and no new degrees of freedom are added to the system. It is effective as long as the proper choice of the contacting penalty stiffness keeps the stability of the system. Early work by Hallquist [28] for two-dimensional sliding contact (master/slave slide lines) led to the establishment of the more general three-dimensional algorithms that are in current use. Given the nature of sliding contact, this approach is most effective in the explicit finite element codes [25], [26], [27]. In its present form, the penalty method with master/slave surfaces is applicable to 3-D problems which include friction.

However, the penalty function method requires a penalty stiffness to be determined for each contacting node. The stability of the contact interference and contact stress distribution over the contact region largely depend on the successful choice of the contact stiffness α. In the master-slave searching algorithm, the accepted automatic method for determining the penalty stiffness is based on the geometry and material properties of the elements associated with the master surface.

$$\alpha = \frac{\beta}{V}(KA_m^2) \tag{1-17}$$

where K is material bulk modulus of the element of the master segment, A_m is area of the master segment, V is volume of the element associated with master segment, and β is a

dimensionless scale factor. The contact interference force then obtained by the product of the penetration and the stiffness. This method successfully overcomes the problem of the stability of the numerical time integration while requiring only one user defined constant.

1.7 Limitation of Automatic Penalty Stiffness Method

Although the automatic penalty stiffness method coupled with master-slave searching approach successfully simulates most of 3-D contact cases, it has a major disadvantage, that is, whenever the mesh of the slave surface is not uniform with that of master surface, a higher stress will occur at such contacting regions. Also, the unexpected higher contact forces and stress will distribute along the corners and edges of slave contact surfaces, this is called the stress edge effect. The reason for the stress edge effect is that the value of the contact force acting on the slave nodes is proportional to the geometry and material property of the master surface, but the transient response of each slave node is based on the structural and inertial property of the slave node itself. Furthermore, the resulting nonuniform distribution of stress over the contacting surface sometimes may cause unexpected noise or vibration. This may even affect the stability of the system in the dynamic transient solution if stress oscillates over the yield stress of the elastic-plastic materials.

1.8 Objectives of this Thesis

The objective of thesis is to overcome the limitation of the automatic penalty stiffness method, which sometimes may cause the high stress distribution along the edge

over the contact region. This requires development of a new contact stiffness model and its implementation into a finite element code to test its capabilities and computation efficiency. Also, application of the finite element code to selection of cases is required to compare the results of the old and new methods, and to verify the effectiveness of the new model.

1.9 Outline of this Thesis

The thesis includes five chapters beginning with the introduction which illustrates the nature of the contact problem and importance of finite element solution to the general contact problem. The typical topics of finite element method solving contact problems are reviewed. And the objectives of this thesis are presented with a final brief summary of the outline.

In Chapter two, the formulation of general contact problem is presented. The penalty method with the explicit transient method (central different method) is derived from the physical kinematic conditions and contact restraints are imposed in a closed form. Also, the master-slave algorithm is discussed in the 3-D contacting model. Finally, the friction law is presented and corresponding interface force is applied to the discretized finite element formulation. This chapter is the basis of the penalty method to solve the contact problem with the central difference approach.

In Chapter three, the contact penalty stiffness is discussed in detail as to how it affects the stability of the numerical solution and current methods to select it. However,

the current method to choose the penalty stiffness raises the two questions: the stress edge effect and numerical inaccuracy and instability. In this chapter, the new method to select the penalty stiffness which can overcome such drawbacks is presented and slave area concept is discussed and numerical procedure is demonstrated.

In Chapter four, the selections of examples are demonstrated to verify the effectiveness of the new method in both the theoretical tests and the practical cases. Finally in chapter five, the main conclusions of this thesis are summarized along with some suggestions for the future work.

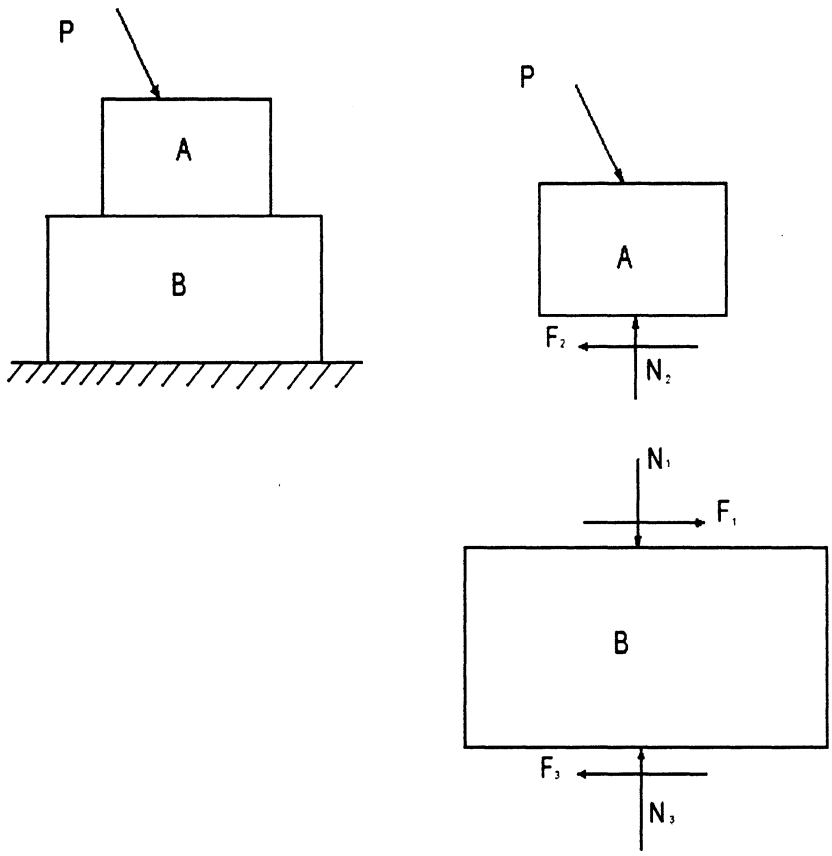

Fig. 1-1 Contact Force in Two Blocks

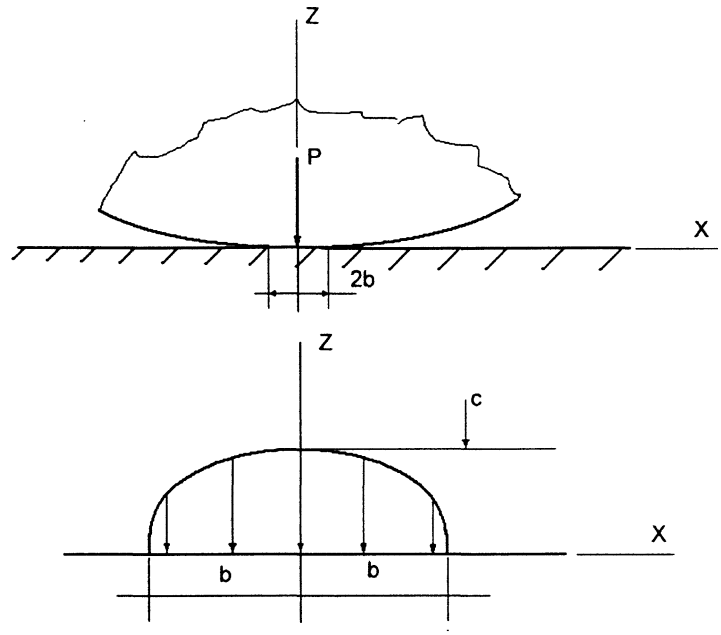

Fig. 1-2 Contact Pressure in Hertzian Contact Theory

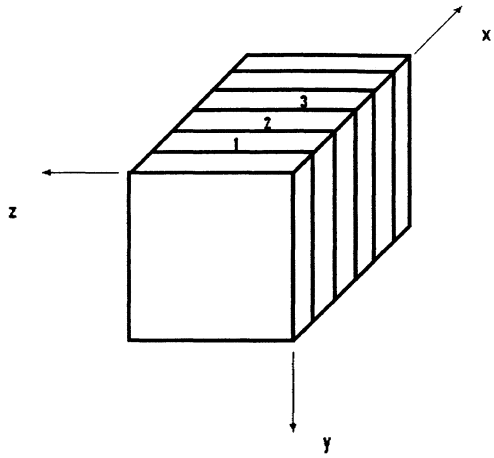

A bucket division in x direction

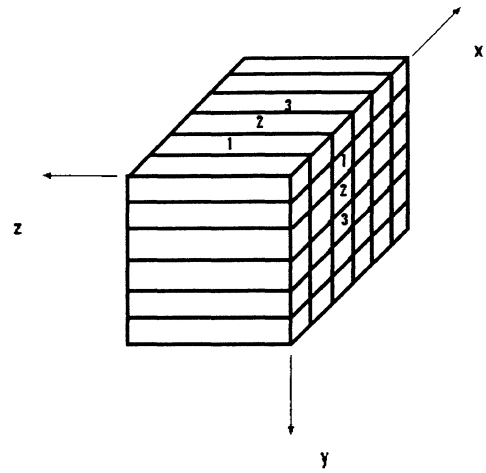

A bucket division in y direction

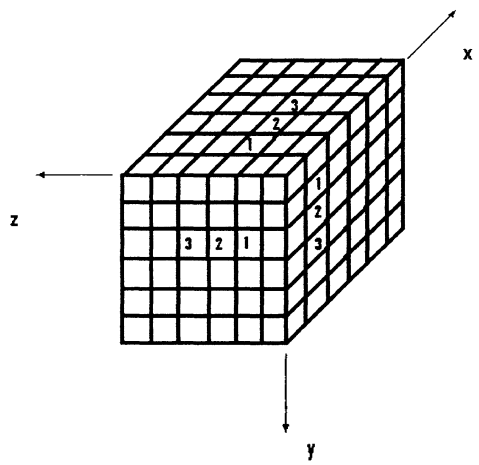

A bucket division in z direction

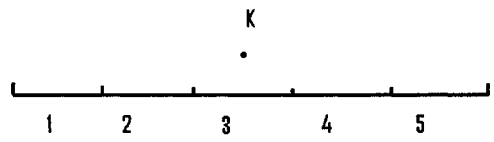

Hitting node K will be examined in bucket 2,3,4

Fig. 1-3 Bucketing Searching

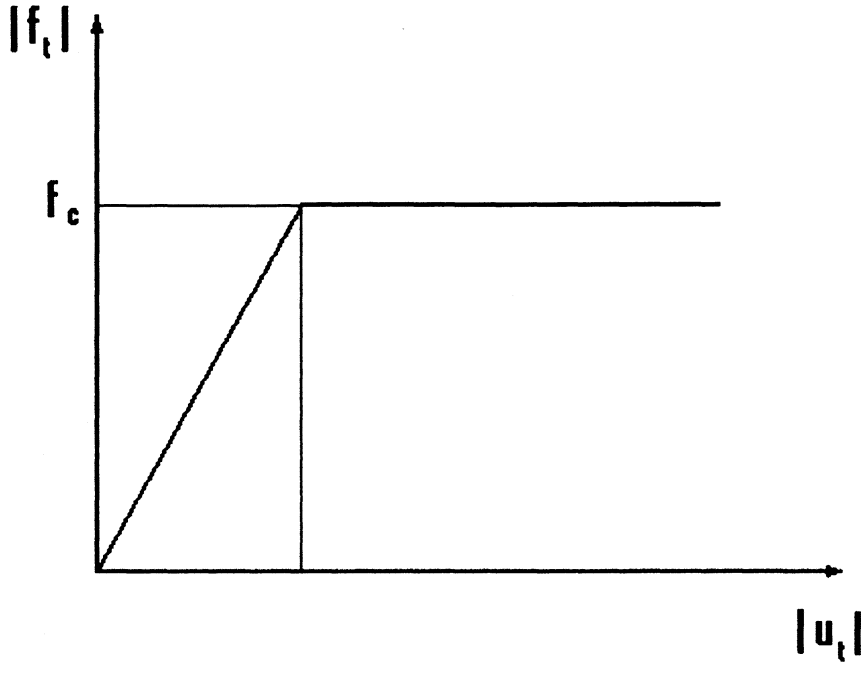

Fig. 1-4 Tangential Contact Forces as a Function of Tangential Displacement in Non-Classic Friction Law

CHAPTER 2

CONTACT PROBLEMS WITH PENALTY METHOD

The Lagrange multiplier method and the penalty method are two main methods to apply the contact constraints on the hitting bodies. The penalty method is extensively used, since its computer implementation is relatively simple, and no more new degrees of freedom are introduced into the system. In this chapter, the mathematical formulation of contact problems with the penalty method to define the constraints is developed and included in the central difference approach for transient problems. Also, the 3-D master-slave (slide-line) contacting searching algorithm is used and the friction force based on the plastic friction model is introduced to account for the sticking and sliding during the contact. Since the formulation is developed in a general form and no restrictions are imposed on the analysis, the whole formulation is suitable for all the 3-D kinematic impact problems, linear or non-linear. The explicit computational method provides the accurate and tractable solution to large-scale problems from the metal forming simulation to the machining simulation, from the crashworthy impact problems to the structural-to-structural interface problems.

2.1 Penalty Method for the Contact Problem

2.1.1 Governing Equations for the Contacting Bodies

The general contacting system may be defined as different regions of contact in one body or more than one contacting body interacting with one another, and interacting contact may occur between two bodies or between separate regions of a single body. For a study model, two bodies can be introduced without losing any generality. Figure 2-1 shows two such bodies brought into contact by the prescribed force applied on the surface of body 2 in a global coordinate system *x, y* and *z*.

2.1.1.1 Equilibrium Condition

For the specific time *t*, the equation of motion of the contacting system can be obtained by applying the momentum principle to the system [41], which indicates that time rate of change of total momentum on a particle equals the vector sum of all external forces. On the contacting bodies, the equilibrium equations of the system can be obtained as:

$$\frac{\partial \sigma_{ji}}{\partial x_j} + F_i = \rho \frac{d\dot{x}_i}{dt} \tag{2-1}$$

where *i* and *j* take on value of 1,2,3 corresponding to *x, y* and *z* directions respectively and summation over repeated indices is implied.

The variables in equation (2-1) are as follows:

σ_{ji} is Cauchy stress components, x_j is the coordinates in *x*, *y* and *z* direction respectively, $\dot{x}_i$ is velocity components, F_i is the body force components and ρ is the mass density of the material.

2.1.1.2 Strain-displacement Relations

According to the infinitesimal strain theory, if the displacement field is such that its first derivative is small and the products of partial derivatives can be ignored, then infinitesimal strain tensor is given by

$$\varepsilon_{ij} = \frac{1}{2}(u_{i,j} + u_{j,i}) \tag{2-2}$$

where the comma indicates differentiation such that $u_{i,j}$ is partial derivative of u_i with respect to x_j.

2.1.1.3 Constitutive Equation (Stress-strain Relations)

A constitutive equation associates the stress with strain in deformed bodies. And such relation totally depends on the property of materials. For a fully isotropic material, elastic properties are the same in all directions. The Hooke's law governs such relations as:

$$\sigma_{ij} = \lambda\delta_{ij}\varepsilon_{kk} + 2\mu e_{ij} \tag{2-3}$$

where ε_{kk} is hydrostatic components of the strain, e_{ij} is deviatoric components of the strain, δ_{ij} is the Kronecker's delta, and λ, μ are Lame constants defined as

$$\lambda = \frac{E\nu}{(1+\nu)(1-2\nu)} \quad \mu = \frac{E}{2(1+\nu)} \tag{2-4}$$

In equation (2-4), E is Young's modulus and ν is Poisson's ratio.

For the elastic-plastic material, an incremental stress-strain relation will be used in the range of plastic state according to the plasticity theory [42].

$$\{d\sigma\} = [E]\{d\varepsilon^e\} = [E](\{d\varepsilon\} - \{d\varepsilon^p\}) \tag{2-5}$$

where $\{d\sigma\}$ is the stress increment, $\{d\varepsilon^e\}$ is the elastic strain increment, $\{d\varepsilon\}$ is total strain increment and $\{d\varepsilon^p\}$ is plastic strain increment.

By applying the associated flow rule of plasticity for the ductile metal, the plastic strain increment $\{d\varepsilon^p\}$ can be expressed as

$$\{d\varepsilon^p\} = \left\{\frac{\partial F}{\partial \sigma}\right\} d\lambda \qquad d\lambda = \{C_\lambda\}\{d\varepsilon\} \tag{2-6}$$

where $d\lambda$ is a scalar called plastic multiplier, F is the yield function which is a function of stress $\{\sigma\}$, W_p is plastic work and α is a hardening parameter given by

$$F(\sigma, \alpha, W_p) = 0 \tag{2-7}$$

According to the yield criterion, to satisfy the constitutive law, dF must be no greater than zero ($dF \leq 0$), or in other words, the stress component can not overpass the yield surface. The mathematical expression of yield criterion is as follows:

$$dF = \left\{\frac{\partial F}{\partial \sigma}\right\}\{\sigma\} + \left\{\frac{\partial F}{\partial \alpha}\right\}\{\alpha\} + \left\{\frac{\partial F}{\partial W_p}\right\} dW_p = 0 \tag{2-8}$$

The combination of equation (2-6), (2-7) and (2-8) gives the way of stress increment calculation when material enters the regime of plasticity. The finite element method to calculate the stress for the elastic-plastic material can be found in [15] and [16].

2.1.1.4 Continuity Conditions

The contacting bodies must satisfy the continuity condition of motion which is given as in [41].

$$\dot{\rho} + \rho \frac{\partial \dot{x}_i}{\partial x_i} = 0 \tag{2-9}$$

In absence of mass transport, the continuity equation is given as:

$$\rho^t V^t = \rho V \tag{2-10}$$

where ρ^t, V^t, ρ, and V are the density and volume at time t and at initial configuration respectively.

2.1.1.5 Boundary Conditions

The contacting bodies must satisfy the kinematic boundary condition and traction boundary condition at time t on the boundaries.

$$u_i^t = d_i^t \qquad \sigma_{ij} n_j = P_i \tag{2-11}$$

where d_i^t is imposed displacement at time t, n_j is unit outward normal to the boundaries and P_i is the tractions applied to contacting bodies.

2.1.1.6 Contact Conditions

For a pair of contacting bodies (Fig. 2-1), a jump condition must be satisfied along the contact discontinuities as:

$$(\sigma_{ij}^{+} - \sigma_{ij}^{-}) n_j = 0 \qquad \text{on boundary} \tag{2-12}$$

where n_j denotes the normal vector of the contacting bodies, $\sigma_{ij}^{+}, \sigma_{ij}^{-}$ are the stress component on the contact surface, and the superscripts "+" and "-" denote the two sides of a contact surface representing body 1 and body 2.

2.1.2 Discretization of Governing Equations

The previous section defines the differential equations and boundary conditions which are called the strong form governing the conditions for the contacting system. The analytical solution for differential equations rarely can be achieved in the contact problem

because of the complicated geometric configuration and contacting constraints. An integral expression (weak form) which implicitly contains the differential equations coupled with numerical techniques provides the possibility to solve such problems. This is the basis of the Finite Element Method. Typically, there are two ways [15] to get the discretized governing equation in Finite Element Methods: Variational Formulation Method and Weighted Residual Method. The Variational formulation is based on the principle of stationary potential energy which has been discussed in Chapter one. Here, the weighted residual method (Galerkin Method) is used to derive the discretized governing equation for the contact problem since the equilibrium and boundary conditions may be considered directly without the need to derive the functional of deformed contact bodies for the variational formulation method. The weighted residual method provides an approximate solution for a governing differential equation whose exact solution is difficult to determine. Suppose for an arbitrary physical system, the governing equation and boundary condition are symbolized as

$$Du - f = 0 \qquad \text{in domain V}$$

$$Bu - g = 0 \qquad \text{on boundary S of V} \tag{2-13}$$

If an approximate solution $\bar{u}$ can be found to make the residual of equation (2-13) small enough, then $\bar{u}$ can be used to project the exact solution of the equation. Normally, $\bar{u}$ interpolates as a polynomial function, $\bar{u} = u(a, x)$. For the specific a, the residual may

vanish for some value of x, but they are not zero for all x, except when $\bar{u}$ is the exact solution.

The equation governing the dynamic response of the contacting bodies can be directly derived by using the Galerkin method of weighted residuals [15]. For the contacting bodies, the residual function for the equilibrium equation (equation 2-1) and boundary and contacting conditions (equation 2-9, equation 2-11) can be expressed in the weak form as

$$\begin{aligned} R &= R_v + R_b = 0 \\ &= \int_v \bar{N}\left[\rho\frac{d\dot{\bar{x}}_i}{dt} - \frac{\partial\bar{\sigma}_{ij}}{\partial x_j} - F_i\right]dV - \int_b \bar{N}(\bar{\sigma}_{ij}n_j - P_i)ds + \int_b \bar{N}(\bar{\sigma}_{ij}^{+} - \bar{\sigma}_{ij}^{-})n_j ds \end{aligned} \tag{2-14}$$

where $\bar{N}$ is a weighting function, $\dot{\bar{x}}$ and $\bar{\sigma}_{ij}$ are the approximation function of the $\dot{x}_i$ and σ_{ij} respectively.

Since $\int_v \bar{N}\frac{\partial\bar{\sigma}_{ij}}{\partial x_j}dV = \int_v \frac{\partial(\bar{N}\bar{\sigma}_{ij})}{\partial x_j}dV - \int_v \frac{\partial\bar{N}}{\partial x_j}\bar{\sigma}_{ij}dV$

and from Gauss's Theorem, the integral of the divergence of vector over a volume bounded by a closed surface is equal to the integral of the outer normal component of the vector over the closed surface,

$$\int_v \frac{\partial(\bar{N}\bar{\sigma}_{ij})}{\partial x_j}dV = \int_s (\bar{N}\bar{\sigma}_{ij})n_j ds \tag{2-15}$$

Substituting equations (2-15) into equation (2-14), the weighted residual becomes

$$R = \int_v \overline{N}\rho \frac{d\dot{\overline{x}}_i}{dt} dV + \int_v \frac{\partial \overline{N}}{\partial x_j} \overline{\sigma}_{ij} dV - \int_b \overline{N} F_i dV - \int_b \overline{N} P ds = 0 \tag{2-16}$$

For all the elements, the equation at time t becomes

$$\sum_{k=1}^{NE} [\int_{v_k} \overline{N}^k \rho \frac{d\dot{\overline{x}}_i}{dt} dV + \int_{v_k} \frac{\partial \overline{N}^k}{\partial x_j} \overline{\sigma}_{ij}^k dV - \int_{b_k} \overline{N}^k F_i^k dV - \int_{b_k} \overline{N}^k P_i^k ds] = 0 \tag{2-17}$$

If the weighting function $\overline{N}$ is chosen the same as the interpolation function for the displacement field, velocity field and stress field, then

$$\dot{\overline{x}}_i = \sum_{j=1}^{n} N_j^k \dot{x}_i^j \tag{2-18}$$

and the discretized governing equation will take the form

$$\sum_{k=1}^{NE} \left[\int_{v_k} \rho N^T N dV \frac{d\dot{x}}{dt} + \int_{v_k} B^T \sigma dV - \int_{v_k} N^T F dV - \int_{b_k} N^T P ds \right] = 0 \tag{2-19}$$

The discretization of governing equations for the dynamic contact analysis can be rewritten in a form as

$$M \frac{d\dot{x}}{dt} + F_{\text{int}}^t = F_{ext}^t \tag{2-20}$$

where the mass matrix are defined as

$$M = \sum_{k=1}^{NE}\left[\int_{v_k} \rho N^T N dV\right] \tag{2-21}$$

and internal force and external force are defined as

$$F_{\text{int}}^t = \sum_{k=1}^{NE}\left[\int_{v_k} B^T \sigma dV\right] \tag{2-22}$$

$$F_{ext}^t = \sum_{k=1}^{NE}\left[\int_{v_k} N^T F dV + \int_{b_k} N^T P ds\right] \tag{2-23}$$

2.1.3 Contact Restraints in the Penalty Method

As discussed earlier, the contact problem is characterized by contact restraints which must be imposed on contacting boundaries when the contact occurs. In the penalty method, penalty forces as the contact constraints will apply to contacting bodies when two bodies come into contact. The contact constraint equations are introduced into the governing equation through the penalty force f_p as follows

$$f_p = \alpha\delta = \alpha\int_b (u_n - \delta_d) u_n db \tag{2-24}$$

where α is the contacting penalty stiffness, which will be discussed in detail in next chapter, u_n is a vector of displacement normal to the contact boundary b_c, and δ_d is the initial gap between the contact surfaces.

Equation (2-20) coupled with contact penalty constraint equation (2-24), provides a simple implementation for the contact problem when the contact occurs. The resulting equation of motion including the contact force is

$$\frac{d\dot{x}}{dt} = M^{-1}\left[F_{ext}^{t} - F_{\text{int}}^{t} + f_{p}\right] \tag{2-25}$$

2.2 Master-Slave Searching Algorithm

In the solution of the contact problem, the searching procedure to locate hitting nodes and potential contacting targets is very important since it will determine the contact constraint force and will influence the efficiency of the numerical solution. The master-slave algorithm provides an efficient way to incorporate the 3-D contact /impact surface undergoing the separation and overlap. The contacting region is described in terms of a master-slave pair of surfaces (Fig. 2-2). One surface is designated as the master surface and the other as the slave surface. In this contact searching algorithm, the slave surface (hitting boundary) and master surface (the target boundary) are specified prior to the solution of the problem. Only the predefined contact nodes on the slave surface (slave nodes) are checked against the contact segment on the master surface to search contacting nodes of the hitting boundary. Undefined nodes are ignored in the procedure of searching.

2.2.1 Master Segment Searching

In contact searching, slave nodes are tested against the corresponding master segment, and if any penetration is detected, the contacting constraint condition (equation 2-24) is activated during the current iteration and contact force is applied to the contacting slave nodes and master segment. The searching procedures consists of four main steps:

1) Search the closest master segment for specific nodes.

2) Test for the penetration and determine the slave node penetration point on the master surface.

3) Calculate and restore the interface force.

4) Modify of system internal force and friction force to account for contact conditions

Of all the steps for the contacting search, the search for the master segment closest to the slave node is the most important. Prior to testing for contact, a search is performed for the master surface in proximity to the slave node which includes two main basic steps:

1) Find the closest master node n_m to the slave node n_s

2) Determine which of the master surfaces associated to n_m is closest to n_s

In application of searching, a hitting node must not pass more than one master surface in one time step. Otherwise, the algorithm may lose track of which master segments are near hitting node and contact will not be detected.

For each master segment, a territory is defined as shown in (Fig. 2-3). By definition, the territory of master segment is defined by domain which is created by the master nodes in the plane. The segment is defined to have a positive side and negative side. The positive side of the master segment is the side on which contact may occur. The definition of the positive side is arbitrary as long as the normal vector of the master segment is in opposite direction of the slave segment.

A slave node is assumed to be in contact with master segment if following condition is satisfied:

$$-\delta_p \leq \delta \leq \delta_d \tag{2-26}$$

where δ_d, δ_p are controlled distance and controlled penetration for the contact respectively, and δ is the penetration function of slave node to the master segment. The control distance δ_d can be set to zero or a non-zero value which accounts for the thickness of shell elements when the contact occurs. The control penetration δ_p is discussed in detail in the next chapter.

After the above condition is determined, the following test must be conducted on master surface connected to n_m:

1) Test hitting slave node in the domain of the corresponding closest master segment (Fig.2-4)

$$\begin{aligned}&(\vec{A}\times\vec{S}_{i+1})\cdot(\vec{S}_i\times\vec{S}_{i+1})>0\\&(\vec{S}_i\times\vec{A})\cdot(\vec{S}_i\times\vec{S}_{i+1})>0\\&(\vec{S}_i\times\vec{A})\cdot(\vec{A}\times\vec{S}_{i+1})>0\end{aligned} \tag{2-27}$$

where $\vec{S}_i, \vec{S}_{i+1}$ are the master segment edge vectors, $\vec{E}$ is vector from master node n_m to slave node n_s and $\vec{A}$ is projection of vector $\vec{E}$ onto master segment.

At least, two of these three conditions must be satisfied to ensure the slave node either n_s lies in the master segment M_i or on one of the edges.

2) In some cases, more than one master segment satisfies the above inequality. For instance, the slave node lies in the corner of the two master segments which is perpendicular to each other (Fig. 2-5). In this case, a surficial contact test is needed. The minimum normal surficial distance is used to determine the candidate master segment.

3) In other cases, the slave node or its projection onto the master segment lies on the edge of the master segments. In this case, the following equation is checked.

$$\left[\frac{\vec{A}\cdot\vec{S}_i}{|\vec{S}_i|}\right]=\max_{i=1,NM}\left[\frac{\vec{A}\cdot\vec{S}_i}{|\vec{S}_i|}\right] \tag{2-28}$$

where NM is the number of master segments related to the master n_m

The segment edge $\vec{S}_i$ corresponding to the maximum value is the required intersection and the master segment containing edge $\vec{S}_i$ will be the target segment.

2.2.2 Interface Contact Forces

Once the above searching phase is complete and corresponding master segment and slave node pairs are determined at time *t*, the contact conditions of slave node with the master segment are tested with:

$$\delta < 0 \quad \delta = \bar{E} \bullet \bar{b} \tag{2-29}$$

where $\bar{b}$ is the average normal of master segment.

When penetration is detected for the specific hitting node, the interface forces are applied to this slave node and master segment according to the equation (2-24).

$$f_p = \alpha\delta$$

The discretized forms of the interface forces are as follows:

1) Interface forces at the slave node for the corresponding master segment

$$F_s = -\delta\alpha \begin{Bmatrix} b_1 \\ b_2 \\ b_3 \end{Bmatrix} \tag{2-30}$$

2) Interface forces at the master segment node *j*

$$F_{m_j} = \delta\alpha N_j \begin{Bmatrix} b_1 \\ b_2 \\ b_3 \end{Bmatrix} \tag{2-31}$$

where N_j are the bi-linear interpolation functions for the master segment.

For the slave node, the interface force is directly added to it once the penetration occurs. Interface forces acting on the master segment must be properly weighted on its nodes. The interpolation function provides the proper distribution of the interface at each node of the master segment. Normally, the bi-linear interpolation function N_j can be used to obtain the simple interpolation of interface force at specific hitting point on the master segment to the four corners of the master segment.

2.3 Friction Model

In the master-slave model, the frictional condition existing between the pair of contacting surfaces is determined by the relative magnitude of the normal and tangential force at the contacting surface. In other words, the tangential friction force is associated with the normal contact force. The friction forces are generated to resist the relative sliding motion of contacting master-slave surface. When the slave nodes are detected to penetrate the master segment, the incremental contact force is evaluated using the penalty stiffness multiplied by the difference in the tangential movement according to

$$\begin{aligned} \Delta\vec{F}_c &= \alpha(\vec{E}^{\,t+\Delta t} - \vec{E}^{\,t}) \\ \vec{F}_c^{\,t+\Delta t} &= \vec{F}_c^{\,t} + \Delta\vec{F}_c \end{aligned} \tag{2-32}$$

The total contact forces must be resolved into normal and tangential components. The resultant tangential forces are then compared to the maximum frictional force μF_N, where μ is the friction coefficient and F_N is the normal force. If the tangential forces are less than μF_N, the slave node keeps sticking along the master segment. Otherwise, the slave node slides relative to the master segment.

For sticking $\mu \mid F_N \mid \geq \mid F_T \mid$

For sliding $\mu \mid F_N \mid < \mid F_T \mid$

The condition for the friction forces can be stated as

$$F_f = \frac{F_T}{\mid F_T \mid} \min(\mid F_T \mid, \mu \mid F_N \mid) \tag{2-33}$$

This friction model is a similar to an elastic-perfectly plastic model. However, in the contact problem, especially in forming processes, the tangential forces along the contacting surface in the large deformation sometimes may exceed the yield shear stress of the material, causing unrealistically high shear stress distribution along the contacting surface. Therefore, a third criterion [26], [27] is used to limit the friction force according to the shear strength of the material. Then, equation (2-33) is augmented to

$$F_f = \frac{F_T}{\mid F_T \mid} \min(\mid F_T \mid, \mu \mid F_N \mid, F_{shear}) \tag{2-34}$$

where the $F_{shear} = \tau A$, τ is the maximum shear stress of the material and A is the area relating force to stress which will be discussed in the next chapter.

2.4 Numerical Explicit Integration

The general equation (equation 2-25) for the contact bodies using the penalty method is a coupled differential equation system called a finite element semidiscretization because, although the displacements are discrete functions of space, its velocity and acceleration are still continuous function of time. For its solution, a numerical integration method is required. The central difference (explicit) method, which is commonly used in engineering analysis, is used for the time explicit integration of the semidiscretized motion equations.

2.4.1 Central Difference Operator

The central difference method [15] approximates velocity and acceleration by expanding the Taylor serious about time t in a mid-step formula to obtain

$$\{\dot{x}\}^{t+\Delta t/2} = \{\dot{x}\}^{t-\Delta t/2} + \Delta t\{\ddot{x}\}^{t} + O(\Delta t^2) \qquad \text{for velocity}$$

$$\{x\}^{t+\Delta t} = \{x\}^{t} + \Delta t\{\dot{x}\}^{t+\Delta t/2} + O(\Delta t^2) \qquad \text{for coordinates} \qquad (2\text{-}35)$$

By ignoring the higher order terms, equation (2-35) becomes

$$\{\dot{x}\}^{t+\Delta t/2} = \{\dot{x}\}^{t-\Delta t/2} + \Delta t\{\ddot{x}\}^{t}$$

$$\{x\}^{t+\Delta t} = \{x\}^t + \Delta t\{\dot{x}\}^{t+\Delta t/2} \tag{2-36}$$

Combining the equation (2-25) with equation (2-36) then,

$$\{\ddot{x}\}^t = M^{-1}[F_{ext}^t - F_{\text{int}}^t + f_p] \tag{2-37}$$

To solve the equation effectively, the diagonal lumped mass is chosen to provide an easily invertible M.

2.4.2 Procedure for the Central Difference Method

1) Calculate the acceleration for the time step t

$$\{\ddot{x}\}^t = M^{-1}[F_{ext}^t - F_{\text{int}}^t + f_p]$$

2) Calculate the current time step Δt

3) Calculate the velocity and acceleration

$$\{\dot{x}\}^{t+\Delta t/2} = \{\dot{x}\}^{t-\Delta t/2} + \Delta t\{\ddot{x}\}^t$$

$$\{x\}^{t+\Delta t} = \{x\}^t + \Delta t\{\dot{x}\}^{t+\Delta t/2}$$

4) Update time $t + \Delta t$

5) Update the internal forces $F_{\text{int}}^{t+\Delta t}$ contact forces $\{f_p\}^{t+\Delta t}$

6) Repeat step1 to step 5

The flow chart is present in the (Fig. 2-7)

2.4.3 Time Stability

In each time step, to keep the stability of the system, the critical time step based on the Courant stability of limited $\Delta t_{cr} \leq 2/\omega_{\max}$ is applied, where $\omega_{\max}$ is the highest frequency of the contacting system. Care must be taken in using the penalty method to solve the contact problem in explicit procedure (central difference method). The penalty method introduces penetration which can be controlled by choosing the penalty stiffness. However, the penalty stiffness contributes to the stiffness matrix but not to the mass matrix, which will cause the frequencies to go up. Therefore, the critical time step will in general decrease when the contact forces are introduced into the system. The amount of such contribution depends on the penalty stiffness. The larger the penalty stiffness, the more the critical time step size is likely to be reduced.

The reduction of time step directly influences the computation time and efficiency. Therefore, the proper selection of the penalty stiffness in the central difference method to ensure that time step Δt is not reduced too much when contact occurs will determine the success of the numerical solution.

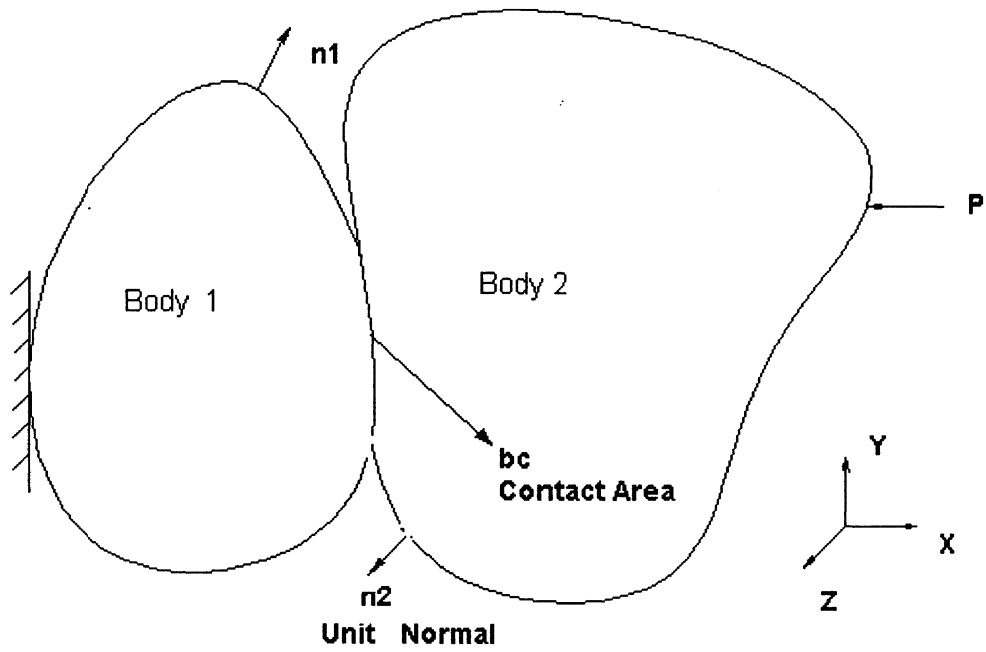

Fig. 2-1 Contact of Arbitrary Bodies

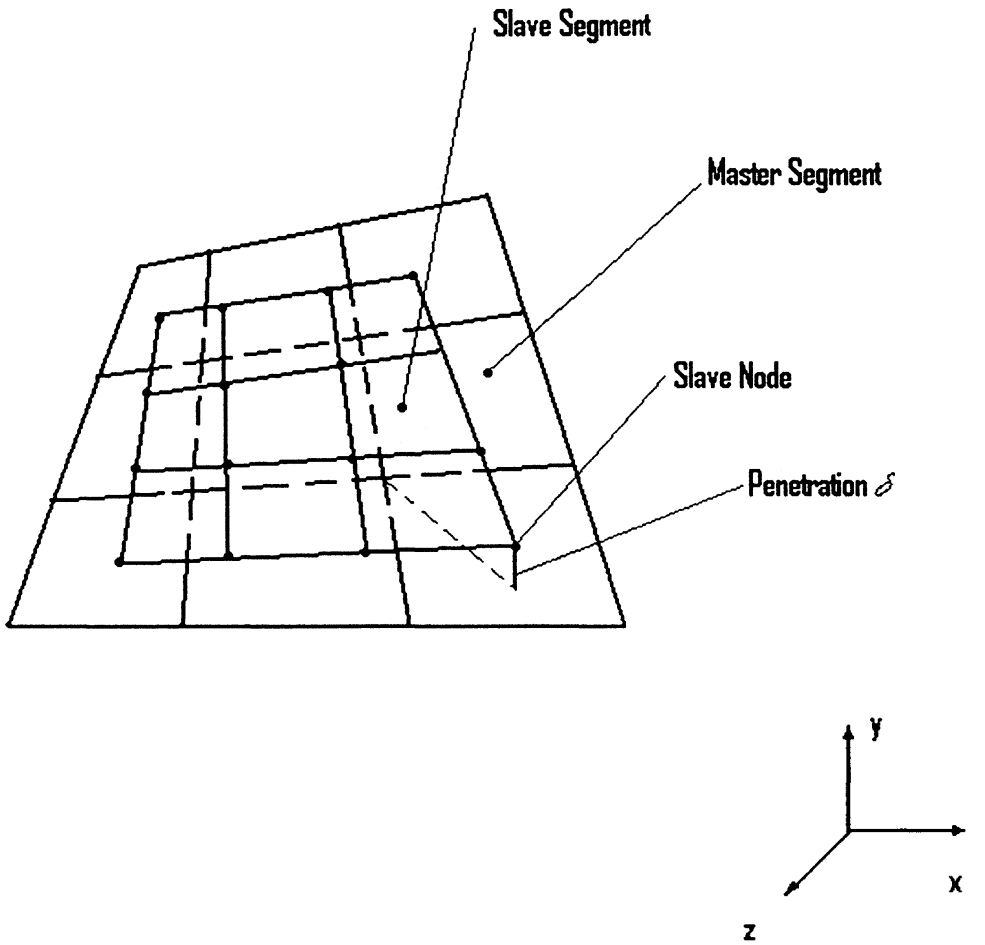

Fig. 2-2 Master-Slave Surface Concept

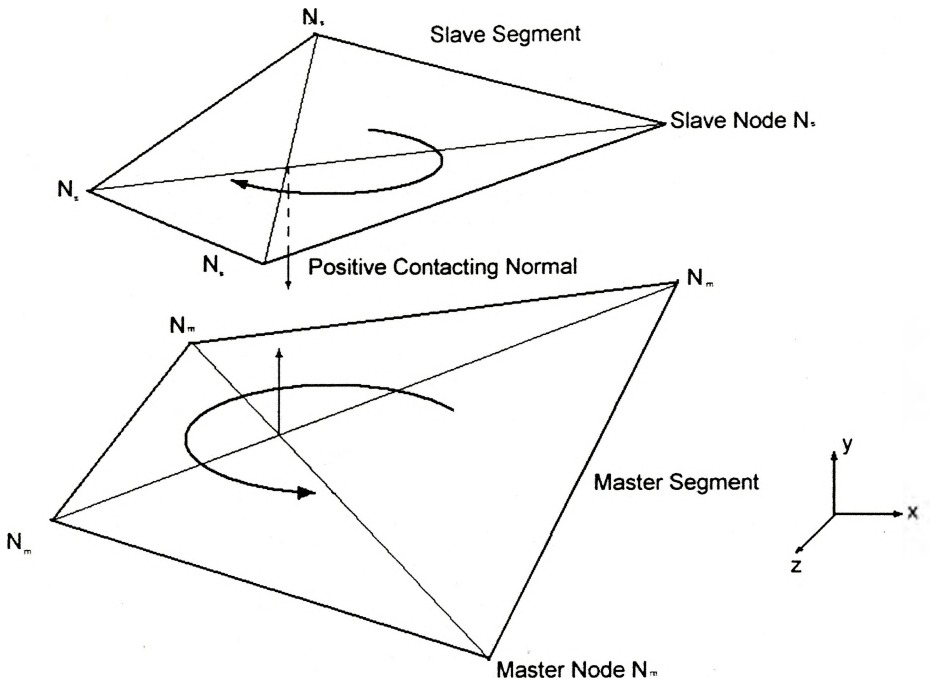

Fig 2-3 Master-Slave Surface Definition

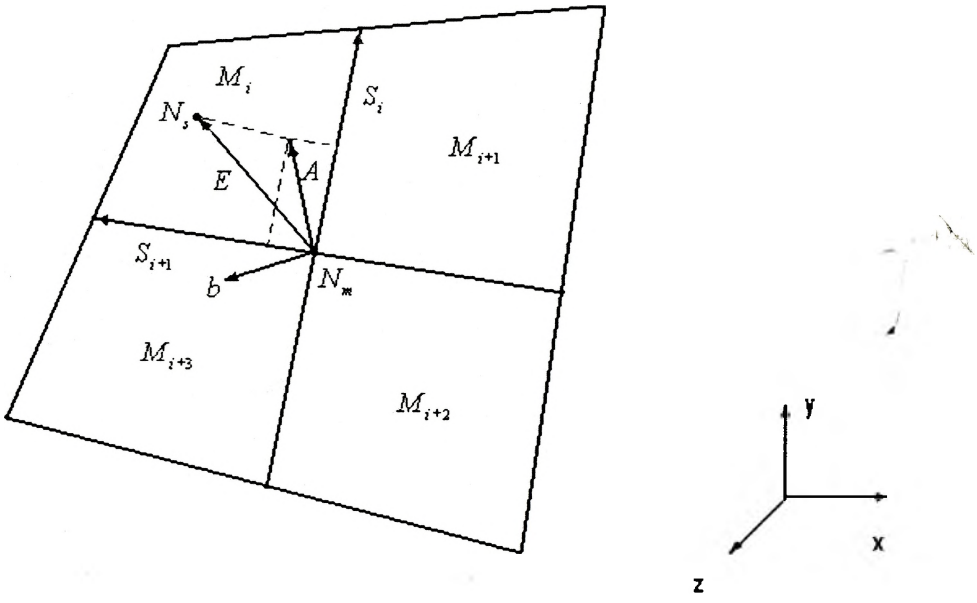

N_s = Slave Node N_m = Master Node

b = Normal Vector of The Master Segment

Fig 2-4 Master Segment Search

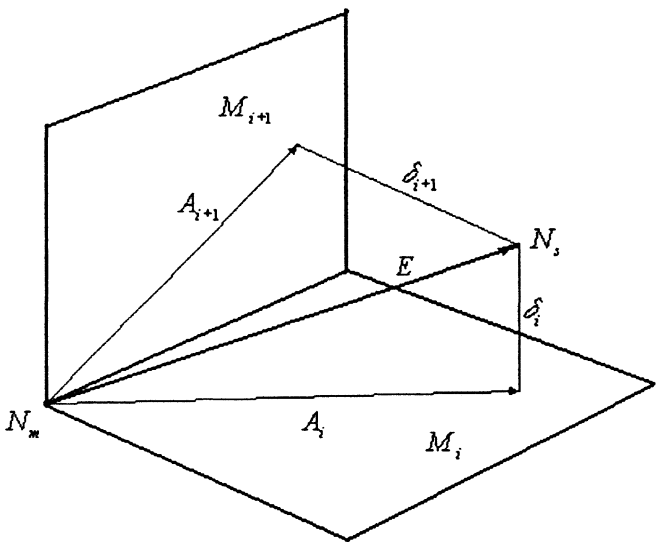

M_{i+1}, M_i = Master Segment Related to Master Node N_m

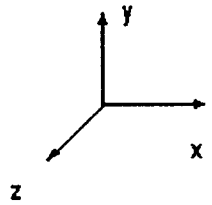

Fig 2-5 Surficial Contact of Master Segment Search

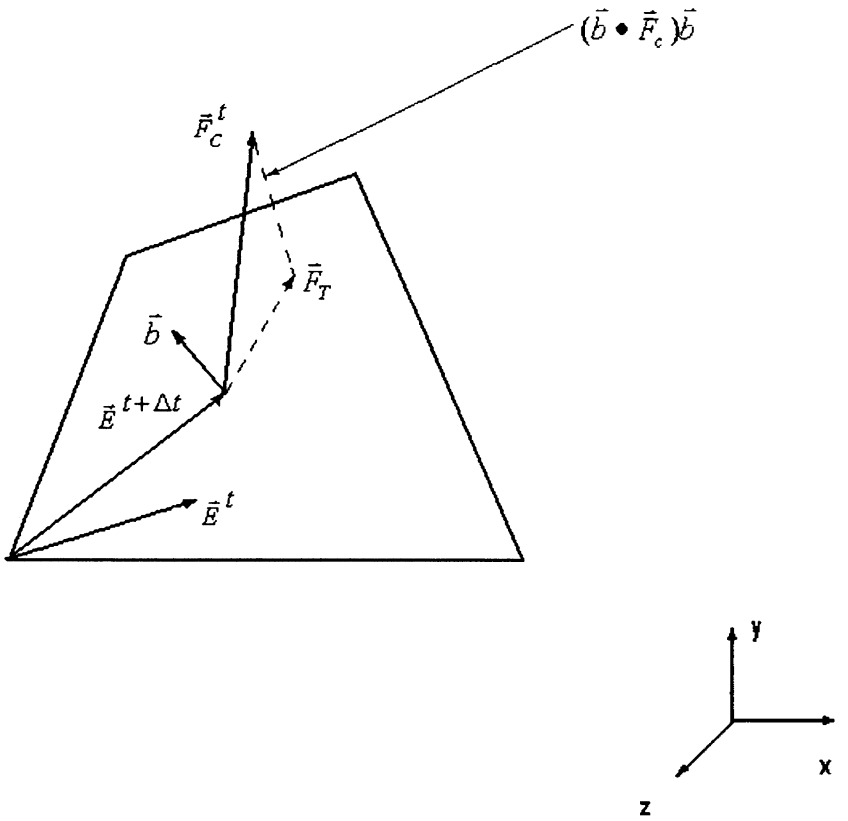

Fig. 2-6 Contact Friction Forces

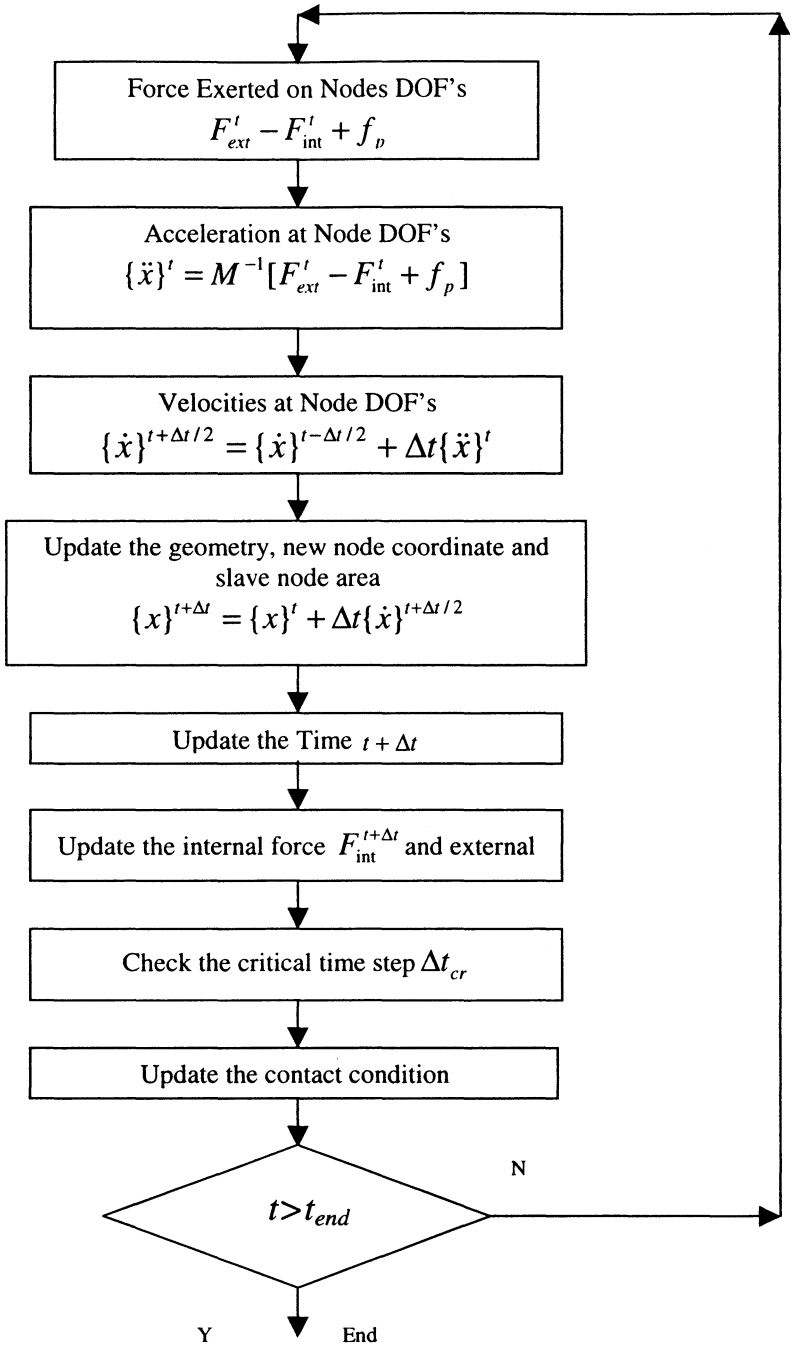

Fig2-7 Flow Chart of the Central Difference Operator

CHAPTER 3

CONTACT PENALTY STIFFNESS

Since the penalty method does not introduce unknown variables to the system, it becomes the most effective way to use the explicit method (central difference method) to do analysis. However, the contact penalty stiffness must be properly chosen to avoid the instability of the system, which is caused by the changing of the system stiffness with the addition of the penalty constraints. In this chapter, the effects of the contact penalty stiffness on calculation efficiency are discussed, and the new contact stiffness model is presented to overcome the drawbacks which are raised by the current approach.

3.1 Penalty Method in the Explicit Method

The success of the penalty method in the explicit approach to solve the contact problem depends on two factors. One is the finite mesh size which will influence the penalty method efficiency in the contact problem analysis. A fine mesh layout of the model means the small length of the elements for analysis. In the central difference method, the stable time step is controlled by the high frequency of the finite element model, which is closely approximated by the upper bound:

$$(\omega_{\max})_e = \frac{2c}{L} \tag{3-1}$$

In equation (3-1), c is the acoustic wave speed which is the speed of the sound traveling through the element, and L is the minimum of the length of element in the finite element model.

Basically, this relates the maximum frequency to the time for a wave to traverse the smallest element. As the size of element goes smaller, the highest frequency of the system goes up, and it needs much smaller time step to keep the stability of the system solution. This results in a large number of time steps during the analysis.

Another factor which influences the efficiency of the penalty method in the explicit procedure is the contact penalty stiffness. The contact stiffness in the penalty method greatly influences the performance of the contact behavior. Since the penetration in the penalty method is controlled by the value of penalty stiffness, the accuracy of the solution using the penalty method largely depends on the choosing of the stiffness. In the explicit analysis, too small penalty stiffness may result in a big penetration and cause unacceptable results. The penalty stiffness must be big enough to control the penetration under a certain desirable level. However, too large penalty stiffness may produce many numerical problems in the solution or even make a solution impractical. In the analysis, an increase in the penalty stiffness results in the decrease of the critical step. As the penalty stiffness goes to infinity, the time step must approach to the zero to keep the stability of the solution. So the successful application of the penalty method in the explicit approach depends on how to properly choose the penalty stiffness to keep the stability and efficiency of the analysis procedure at the same time.

3.2 Automatic Determination of Penalty Stiffness

The problem-dependent characteristics of contact make a good estimate of penalty stiffness difficult. As the contact stiffness α acts as a linear compression spring when the penetration occurs between the master and slave surface, the value of α may reduce the time-step that can be used to guarantee the stability of the explicit time integration. Also, the problem-dependent characteristics make it difficult for the users to properly choose the stiffness.

To overcome such drawbacks, the typical way in [25], [26] and [27] to obtain the penalty stiffness is to relate the stiffness with the geometry and material properties of the master surface. For master surfaces attached to solid elements,

$$\alpha = \frac{\beta}{V}(KA_m^2) \tag{3-2}$$

where K is material bulk modulus of the element of the master segment, A_m is area of the master segment, V is volume of the solid element associated with master segment and β is scale factor (a dimensionless parameter). A commonly used default value of $\beta = 0.1$ is suitable if meshing of master surface is identical to that of slave surface and contacting bodies are of materials with similar stiffness. This contact penalty stiffness applies to the three-dimensional linear continuum hexahedron finite element formulation. For the linear continuum shell element, the penalty stiffness takes form as

$$\alpha = \beta K_k \left[\frac{A_k}{h_k}, \frac{A_k}{|\vec{V}_{kn}|}, \frac{A_k}{|\vec{V}_{ml}|} \right]_{\min} \tag{3-3}$$

where h_k is the thickness of shell element associated the master segment k, and $\vec{V}_{kn}, \vec{V}_{ml}$ are the two lengths of the diagonals of the shell element of the master segment k.

Since the penalty stiffness of equation (3-2) and (3-3) is based on the geometry and material properties of the element which is associated with the master segment, the magnitude of the time step remains almost unchanged for the iteration in the explicit method if the meshing of master surface and slave surface is uniform. Thus, it will not affect the stability of the system and the efficiency of the solution. During each time step, after obtaining the penalty stiffness, the interacting contact forces are then obtained by the product of penetration and this stiffness, which usually provides acceptable contact characteristics without disrupting the conditional stability of explicit time integration scheme.

3.3 Problems of the Automatic Penalty Stiffness

The automatic determination of penalty stiffness works well for most of the contact problems. However, this method of determining contact stiffness raises two problems.

1) Nonuniform contact pressure occurs at edges or regions of mesh transition (fig. 3-1). Since the interface forces are associated with the geometry and mesh size of the master surface, the corresponding force acting on the each slave node will be

proportional to the master area property, but the structural and inertial properties of the slave nodes depend on the slave surface geometry. This will cause nonuniform response of the slave nodes to the corresponding contact forces such that stress will be higher at corners and edges of a slave surface, the stress edge effect. Similar nonuniformity can also occur at mesh transitions for the same reason as mentioned above. The occurrence of higher stress at edges can cause premature plastic deformation even when nominal contact pressure should result in elastic response. In such cases, equilibrium may be difficult to reach and the contact force may be observed to oscillate.

2) The distribution of friction forces along the contact surfaces can be adversely affected since the stick/slip condition may be erroneously determined due to the nonuniformity in contact pressure arising from point 1 above. The reason for this is that in the master slave searching approach, the friction force is directly associated with the contact force which has been discussed in chapter 2.

3.4 New Contact Stiffness Penalty Model

The new contact stiffness model is developed on the basis of elimination of the stress edge effect over the contact region and reaching the uniform pressure condition along the contact surface even for nonuniform meshing of the master surface. Since the dynamic response of each slave node is proportional to its inertial property, if the interface forces (controlled by the penalty stiffness) can be associated with the mass property of the slave nodes, the response can also be consistent and uniform pressure

condition can be reached without considering the mesh of the master segment. In this thesis, a new method to select the penalty stiffness is developed. Other than to associate the contact penalty stiffness with the corresponding property of master segment, the new stiffness depends on the material property and the geometry of slave surface. It still keeps in mind the need to maintain the stability of the explicit integration. The new contact stiffness is calculated as

$$\alpha = \frac{P_{ref} A_S}{\delta_{ref}} \tag{3-4}$$

where P_{ref} is the reference contact pressure normally defined to be less than the normal yield stress of the material of slave segment, δ_{ref} is the reference penetration corresponding to a contact pressure of P_{ref}, and A_S is the area associated with each slave node.

The concept of A_S is as follows (Fig. 3-2): For the linear continuum quadrilateral elements (solid or shell), the slave node area is a discrete representation of a continuous distribution of the slave surface. The slave node area is obtained by proportionally placing the area of the each element at the nodes that are associated to the element, such that the sum of the slave node area of the element is the total element surface. The sum of all the slave areas for the specific slave node will form the total slave node area for that slave node. For example, the slave node area of node P takes the areas from elements

1,2,3,4. The slave node R will take the area from the element 1and element 4 and Q will only take the area from the element 3.

An efficient calculation of the area of the quadrilateral element is presented by Liu W. K. in [43]. Here, an approximated area calculation of quadrilateral element has been used. It is supposed that four node in the slave segment takes the same amount area that is the quarter of the area of the slave segment. To account for the warped quadrilateral element, the slave segment are divided into two triangles, the sum of the areas of the triangles approximates for the space area of the warped element. The efficiency of the calculation of slave node area in the explicit method is not a problem since a criterion to update the slave node area can be set during the analysis, say, 2 percent or 5 percent of the distortion of the slave area will activate update the slave node area.

Since the contact stiffness in each contact set is associated with the corresponding slave node areas, which are proportional to the value of structural and inertial properties of each slave node under uniform bodies, it is expected that dynamic response for each slave nodes during the contact remains consistent. This will avoid the stress edge effect as mentioned before. At each time iteration, friction forces are also detected and compared with the normal forces, since the friction forces are associated with the motion of the salve node along the master segment, such forces are proportional to the contact forces during the sticking state or to the limiting friction if sliding is going

to happen. So, this method can also keep a uniform friction force distribution along the contacting surface when surfaces are set at the sticking state.

The application of this new method must take into consideration the magnitudes of the reference contact pressure and reference penetration since the reference contact pressure and its associated reference penetration are defined by the users. If the resulting value of α ends up being too small, excessive penetration of slave nodes into the master segment may occur which makes the solutions improper. If the penalty stiffness is too high, the time step required for stability may be prohibitively small in the explicit method and may lead to slow convergence or even makes the solution impractical when the penalty stiffness is much higher than the stiffness of the contact system itself.

3.5 User Perspective

The new approach of selecting the penalty stiffness gives the user more options to control the contact performance than the automatic penalty stiffness. The users have to define the reference penetration and reference contact pressure for each contact set. Since both variables have clear physical meanings according to the actual contact conditions, there should be no difficulty to make such a selection.

For the reference penetration δ_{ref}, it is a problem-dependant parameter. For example, in most cases, it can be a fraction of the element depth below the contact because during the contact, maximum penetration is not expected to pass over one contact element, otherwise it might cause the ill-conditioning of the analysis. Also, it can

be related to geometric tolerance of surface roughness of work piece in machining process since such selection would not affect nominal dimensions and would be consistent with actual situation.

For the reference contact pressure P_{ref}, it should be associated with the material property of the slave surface. For example, the reference contact pressure P_{ref} should be less than the yield stress of the slave element material. Such a definition will limit the contact surface to be undergoing the excessive pressure which may even exceed the yield stress of the contact bodies.

The new way to select the contact stiffness is based on the geometry and material property of the slave surface during each iteration. While the time stability is not any more difficult to reach compared with the automatic penalty stiffness. Care must be taken to consider the time step during the analysis. As discussed earlier, the penalty stiffness can increase the frequency of the system, so the time step will reduce with the introduction of new penalty stiffness. Since the users will control the penalty stiffness, the improper selection of an excessively small reference penetration δ_{ref} or a high reference pressure may greatly reduce the time step. In some circumstances, the compromise between efficiency and accuracy could require careful consideration to get job done. Overall, the new way gives the users more possibilities to control the contact performance.

3.6 Implementation the New Approach into F.E. Code

The new approach to calculate the penalty stiffness described in the preceding sections has been implemented into the explicit module of three dimensional non-linear transient dynamic finite element computer code H3DMAP 6.2. In order to achieve maximum versatility and make it open for further development, H3DMAP has been organized in a modular form. Owing to its open architecture, it is possible to modify the program by simply inserting new modules and adding the new variables to the global array.

3.6.1. Algorithm Data Structure

In the H3DMAP, the contact data structure is set up the contact algorithm data manager (COMMON) subroutine. The addressees which point to the specific location within a single dimension array, A(I), are calculated from the problem input parameters. All the program array variables are contained in this array. The amount of memory required varies with the size of the problem considered. For new variables, such as the reference penetration, reference pressure, maximum shear stress and control parameter, the unique addresses must be assigned to them by predefining the "A" array.

3.6.2. Module Functions

In the H3DMAP, the contact algorithm module fits into the framework of explicit code architecture. The various subroutines, from which the contact algorithm is

comprised, are shown in figure 3-3. The implementation of algorithm occurs in three steps:

1) Contact data input and array initialization

CONMAN: contact algorithm manager which sets up the address of the appropriate variables in global array "A".

Subroutine CONMAN has been expanded to set new addresses to the "A" array for the new variables: reference penetration, reference pressure and maximum shear stress.

CALIN1, CALIN2, CALIN3: reads the contact algorithm control information and master/slave definition for each contact set.

Subroutines CALIN1, CALIN2, CALIN3 have been modified to read the data of new variables.

2) Initialization of contact parameters

CALI1, CALI2: match master surface segments to element sides and initialize the contact search algorithm.

Subroutine CALI1 has been modified to trigger the new penalty stiffness calculation if the control parameter is selected.

3) Solution phase

CAL1: loops over all slave nodes in a contact set, and searches for current closest master segment.

CAL2: checks for penetration of slave nodes into a designated master surface found in search phase (CAL1). For contact, the point of penetration within a segment is found and internal element force vector is updated using calculated interface forces.

The new subroutine SLAVEAREA is added into the EXPRES module. The SLAVEAREA calculates the slave node area and corresponding new penalty stiffness according to the current geometry of slave surface. The new contact stiffness is called by the CAL1 and CAL2 to account for the new interface force calculations. Also the CAL1 and CAL2 have been modified for the new computation of contact forces.

Since H3DMAP is organized in modular form, the other modulars such as nonlinear creep analysis can successfully call the proceeding modified subroutine without any other modifications. Therefore, the new penalty stiffness method has become an additional option available for the general application of the finite element code.

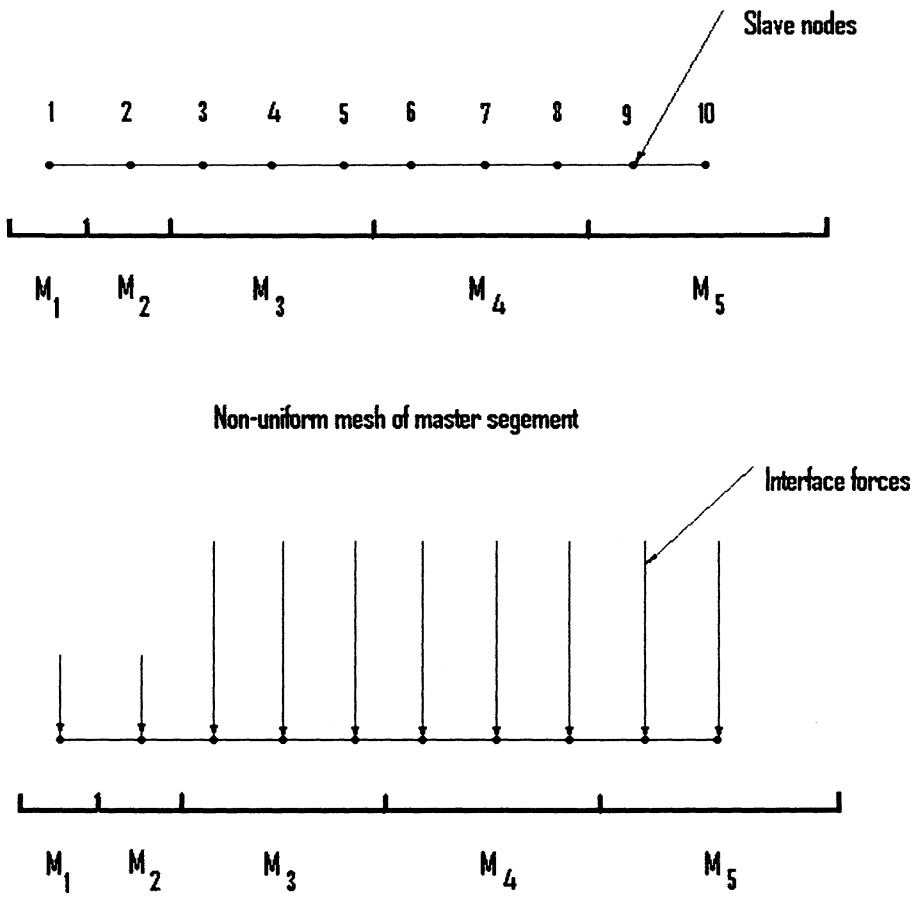

Fig. 3-1 Nonuniform Mesh of Master Segment Causing the Different Interface Force on the Slave Nodes

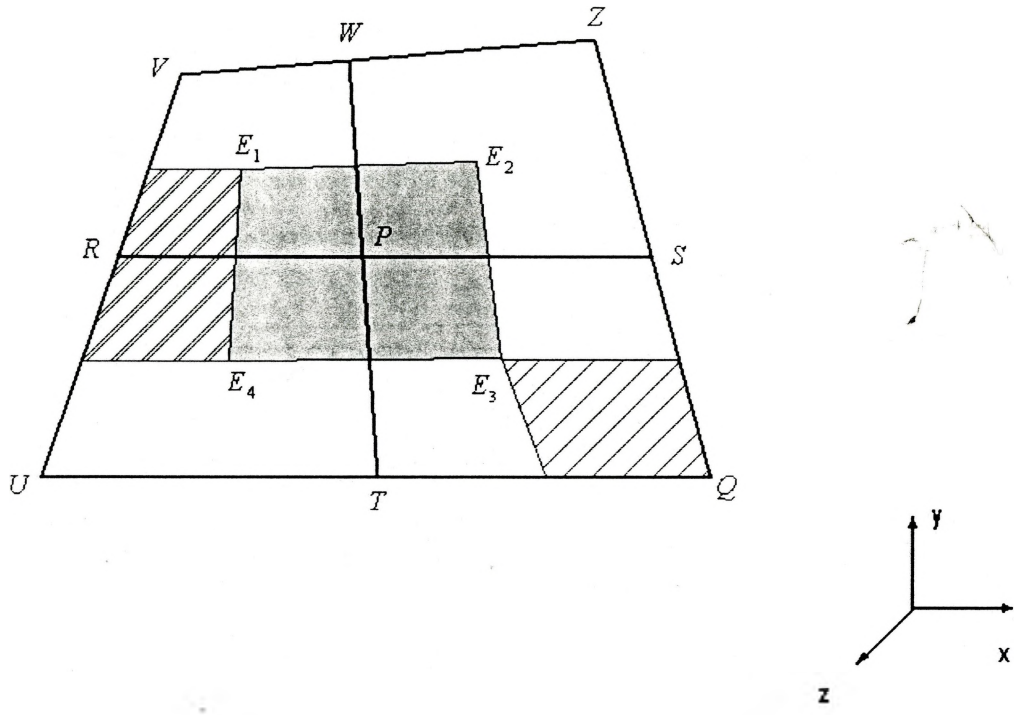

Fig. 3-2 Slave Nodes Area

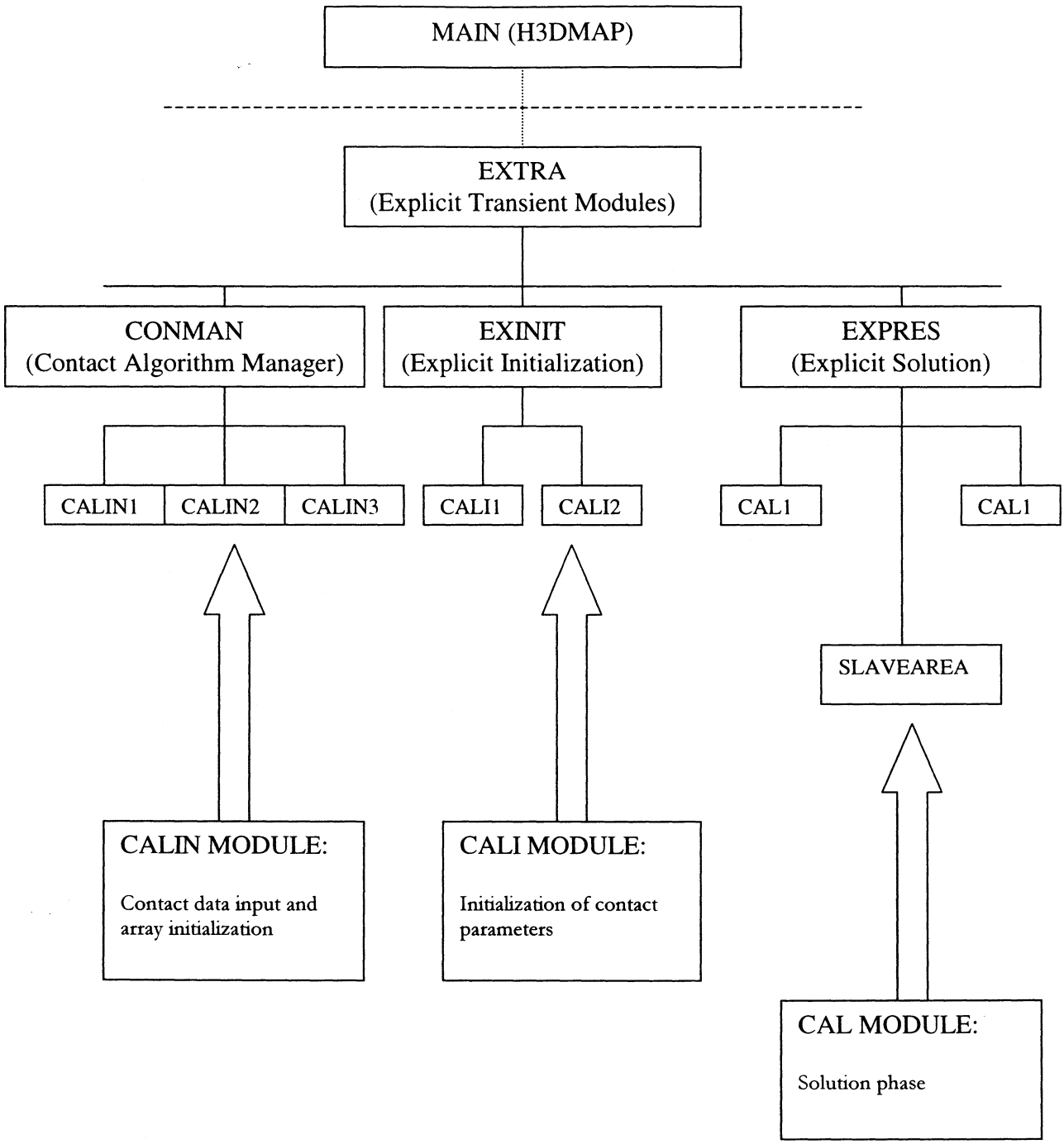

Fig. 3-3 Contact Algorithm Module Structure

CHAPTER 4

EXAMPLES

In this chapter several test cases are presented to compare the effectiveness of the contact stiffness in the new method with that in the old method. Both frictionless and friction models, and uniform meshing and nonuniform meshing models are studied. It should be noted that three of the test cases just present the effectiveness of the new method, so much simplified models are selected to make such comparisons easily and clearly. Also, the two other practical and more complicated examples are presented to show the application of the new method in realistic modeling situations. One case is the clamping simulation during the punching process, which shows how the new method can avoid the numerical noise to keep the stability of the system. The other one is the rolling process which shows the uniform shear stress distribution over the rolled plate in the new method, the results of which are consistent to the analytical solution in the metal forming process [44]. All the examples are performed on the contact algorithm developed for the explicit finite element code H3DMAP [46] with relative modification on the contact stiffness calculation, the method of which is presented in Chapter 3.

4.1 Test Cases

4.1.1 A Cube Block Compression without Friction

4.1.1.1 Finite Element Modeling

A cube block compression test (Fig. 4-1) is used to test the contact algorithm between the shell and solid contact. In the test, the block (0.2x0.2x0.2m cube) is modeled as four solid elements. The compression plate (master surface) is modeled as a single shell element. Such simplification will make comparison relatively easy for two reasons:

1) All the reacting contact stiffness between each slave nodes and master segment will be exactly the same for one single master segment definition during the process of transient response. This makes the slave surface property (the mesh size and material property) the only fact influencing the contacting forces and makes the comparison easy.

2) If the plate is modeled as numerous shell elements, warped shell might occur during contact with initial velocity loading since the reacting contact force is different.This makes the final results incomparable, and single shell avoids such influence.

In this simple test, the initial velocity (5 m/s) in the negative y direction (downward) is applied to the four corners of this single shell element. The top surface of the cube is modeled as slave surface and the bottom is fixed in all directions. As the plate drops down, the contact reaction occurs when the slave nodes penetrate the shell (master segment) and corresponding contact force will apply to the slave nodes and single shell element. The contact force will increase as the penetration goes up, so the kinetic energy of the shell element will reduce until that it bounces back. Also, the contacting force on the slave nodes will cause the deformation of the block (solid element) and internal solid

energy will increase in the range of the elastic plastic field. In this test, the block is modeled as elastic perfectly plastic material and the shell is elastic. The thickness of the shell element is 0.01m. In the new method, the reference contact pressure is set below the yield stress of the solid material, the reference penetration is set at one tenth of the thickness of the element below the contact surface. The transient analysis is done by comparing both methods at a time (0.007 second) well after the single shell element has bounced back. Also, one of the four solid elements is selected to present its stress response during the whole process. Such analysis would not lose the generalization since the four elements show the same dynamic response during the compression.

4.1.1.2 Results and Discussion

The comparison of Von Mises stress in both methods (the contact stiffness defined by the master property and contact stiffness defined by the slave node property) (Fig. 4-2 and Fig. 4-3) at the time of 0.007 shows a great difference of stress distribution on the contact surface. For the method of which the stiffness is defined by the master geometry, the highest stress occurs on the four corners and the center of block shows the lowest stress, the typical stress edge effect. The new method pictured in figure 4-3 shows a very uniform stress distribution over the contact surface since the transient response of the slave nodes caused by the contact force is proportional to the structural and inertial configuration of the slave nodes and that is also consistent with analytical solution of stress distribution for the non-friction model. The quantitative comparison of the two methods is difficult since the penalty stiffness cannot be precisely matched. It should be

noticed that since the transient solution is used on this test, the stress on the contact surface should vary with the different time interval but at the specific time, the response of the contacting force on the slave nodes should be exactly the same for all the nodes in this frictionless model no mater where the slave nodes is located.

The comparisons of stress dynamic response of one of the four solid elements (element 3) during the whole contacting process show more interesting results. In figure 4-4 and figure 4-5, the von Mises stress shows a different variation for both methods during the period of 0.007 second. For the old method, the von Mises stress keeps vibrating with different amount of amplitude after the plate bounces back when the contact is finished. Such results are caused by the difference of stress distribution on the four corners and the stress at the center even in one element. Such unbalanced stress dynamic response in one element will cause the numerical noise even after the contact finish since the nodes fail to reach equilibrium for the transient analysis. In the new method, the stress amplitude during the response is almost the same since all nodes in each element keep the same response because of the new way of applying the contact force.

4.1.2 A Cube Block Compression with Nonuniform Meshing and without Friction

4.1.2.1 Finite Element Modeling

The model of this test is similar to the previous one but the solid block is modeled as solid element with bias meshing (Fig. 4-6) and elastic plastic material is used in this

case. The block is modeled as elastic plastic material with the yielding 500 MPa. The shell is elastic with the thickness 0.01m. In the new method, the reference contact pressure sets as 6 MPa and the reference penetration 0.003m. The loading is controlled by the constant velocity applied (5 m/s) to the four corners of the plate in the negative y direction (downward) during the first 0.058 second. After that, the constant velocity reduces smoothly to zero. Such loading will maintain the desired displacement control. Also, the transient analysis is done by comparing both methods at a time (0.007 second). Since biased meshing is used for the slave surface, the stress distribution will be partly affected by such mesh patterns.

4.1.2.2 Results and Discussion

Compared to the stress results of the uniform meshing (Fig.4-2), the distribution of Von Mises stress in the figure 4-7 shows an unsymmetrical distribution. The high stress occurring at the finer meshed elements (the right top side of the block) is almost five times the stress at the center, and the stress on the left side is below the stress on the right side. The meshing pattern of the slave surface accounts for such a difference since the slave nodes will take the same amount of contacting force from the single master shell element but the masses of the slave nodes are not uniform. It is obvious that in the old method, meshing is an important factor for the stress and the slave surface meshing size, and the meshing transition will affect the stress distribution over the contact surface. Taking a look at the stress distribution on the whole contact surface, note that the model

should respond elastically for the given displacement, but stress in the old method (Fig. 4-7) has encountered some yielding (500 MPa) at the corners with small elements.

The new method pictured in Figure 4-8 shows a very uniform stress distribution over the contact surface, while the slight stress difference along the cube block is due to stress wave propagation from the top surface to bottom due to the explicit transient solution technique which is undamped in these examples. Note that the model correctly responds elastically for the given displacement.

4.1.3 Cube Block Compression with Friction (Uniform Mesh)

4.1.3.1 Finite element modeling

This case (Fig. 4-9) tests the shear stress distribution along the contact surface caused by the friction force. The finite element model is similar to the first test case except the friction coefficient is applied between the single shell and block with the static friction coefficient 0.17 and dynamic friction coefficient 0.13. The material for the solid is still elastic perfectly-plastic and the shell is elastic. The reference contact pressure is set to 80 MPa, and the reference penetration 0.001m. The loading of the test is in two steps:

1) Constant vertical velocity (5m/s) is applied to the four corners of master surface during the first 0.0041second in the negative y direction (downward) and keeps such displacement during the next step loading.

2) Then, constant velocity (5 m/s) in the horizontal direction (x direction) is applied to the shell element.

Such loading can keep a constant displacement on the single shell. Since there is friction between the shell and solid element, horizontal loading will convert to shear stress on the solid contact surface. Examining the shear stress on the top surface of the solid can reveal the different results between the two methods because the shear stress is also associated with motions of the slave nodes, and slave node motion is directly associated with the contact force and contact stiffness as discussed in Chapter 3. In order to get pure shear stress that is completely created by friction, periodic symmetry is applied on the four vertical surfaces of the cube block to constrain any volume change that occurs during the compression stage of loading. In this case, sticking is supposed between the contact surface and the friction coefficient is chosen to avoid relative sliding of the contact surfaces with respect to each other.

4.1.3.2 Results and Discussion

The shear stress plot (Fig. 4-11) of the modified contact stiffness for the friction model shows a uniform stress distribution in the X-Z plane. Since the friction force is directly associated with shear stress and the friction force is proportional to the contact force acting on the slave nodes, it is clear that the suitable values of contact stiffness α have maintained the uniform distribution of the contact pressure necessary for the corresponding uniform shear stress. For the original method (Fig. 4-10), the distribution of the shear stress shows a gradient from the left to the right. This is because the

compression step causes higher stress at the corners and horizontal motion of the master segment creates friction force accounting for the higher accumulated shear stress in the left corner than that in the right side. The stress difference is almost doubled.

Figures 4-12 and 4-13 show the contact force variation in the x direction (the direction of shear) during the whole period of time (0.007) for one of the elements. Such contact force is proportional to the shear stress since it causes the block to shear. Both methods demonstrate the similar trend during the loading period. However, the contact force variation in the new method is smoother during the loading process, this is because the selection of the penalty stiffness accounts for such a uniform distribution in the new method. Also, the magnitude of contact force is incomparable since the method to define the penalty stiffness is different.

4.2 Sample Studies

4.2.1 Clamping Simulation for Punch Test

4.2.1.1 Finite Element Modeling

The punch process is a typical multiple-contact problem with extensive application in the industry. During the process, four sets of contact are introduced: 1) punch and work piece. 2) work piece and die. 3,4) work piece clamping (upper surface with blank holder and bottom surface with the blank holder). In the punch test example previously considered in [47], the clamping of a flat specimen was prone to excessive noise from the contact surfaces which may cause error in the plastic strain accumulation.

The punching process (Fig. 4-14) is modeled as follows: The simulation uses a one quarter model according to the planes of symmetry on the long vertical edge in view in figures 4-14, the left end of the specimen (4x10x.47mm). The punch and die are both modeled as shell elements and the upper blank holder (also shell) clamps the specimen (model as a solid element) in the stage of the clamping by way of the vertical pressure applied to the blank holder which contacts the top surface of the right half of the specimen. Support from below is through contact with a rigid lower die. After the initial clamping is finished, the motion imposed on the punch pushes the punch through the work piece to get deformed shape. During this stage, another two contacts occur: the punch and work piece, work piece and die. The specimen is modeled as variable hardening elastic plastic material with yield stress $\sigma_{ys} = 200$ MPa. And the blank holder is elastic. The vertical pressure is applied to the blank holder to create the clamping force for the initial stage in the punch test.

4.2.1.2 Results and Discussion

As shown in Figure 4-15, the normal stress over the clamped section shows a typical stress edge affect and variation in stress at the mesh transitions when the old method is used. The normal stress distribution of the new method (Fig. 4-16) shows satisfactory results during a constant pressure clamping on the metal. The quite uniform stress distribution along the surface avoids noisy dynamic response and keeps the clamping in a quiet state.

By comparing the contact force (or average pressure) with both methods, it is clear that the original method will cause an inconsistent dynamic response of slave node along the contacting surface due to the contact force applied on the nodes, and system continues to vibrate as it unsuccessfully seeks a suitable equilibrium configuration (Fig. 4-17). On the contrary, Figure 4-18 shows that the new method overcomes such a drawback and the system smoothly reaches a state of stabilization after the loading is finished.

By examining the contact force acting on the punched section through the whole punch procedure (Fig. 4-19 and Fig. 4-20), it is obvious that the contact pressure more smoothly reaches its highest value by using the new method than that of old method. This is because the interface forces acting on the surface of contact elements are more uniform in the new method and the system remains in a state of good equilibrium configuration.

The plastic strain over the working model also shows the difference between the old method and the new method (Fig. 4-21 and Fig. 4-22). In the new method, the plastic strain is more evenly distributed over the punched section than that in the old method since interface force is more uniform with the new method.

4.2.2 Rolling Process

4.2.2.1 Finite Element Modeling

Another sample study is the rolling process simulation. Rolling is a typical contact process which the roller squeezes the metal plate along the direction of

elongation. Since the purpose of the model is to examine the shear stress distribution caused by the friction force, a simplified model is made without consideration of back and front tension and without consideration of the lubrication between the tooling and work piece. A quarter model is defined for the finite element analysis since the rolling plate and the roller is also symmetrical in the *y* direction. In this model (Fig. 4-23) the roller is modeled as an elastic material. The work piece (160x50x18.5mm) is modeled as an elastic plastic material with isotropic hardening. The constant angular velocity 2 radian/s is applied to all the roller nodes. To get rolling process started, the constant force is applied at the right end of the plate for 0.55 second until enough contact surface is reached and friction force can squeeze metal plate forward. In the new method, the reference pressure is set to 70MPa and allowed penetration sets one-tenth the thickness of the contacting slave element. The rolling process is a high friction contact problem since the friction force acts as the driving force to squeeze the plate in the direction of elongation. A high dynamic friction coefficient of 0.4 is chosen in this simulation. Since the friction force between the roller and plate is the main external force, the corresponding shear stress will reflect such contact condition and show the different results of both methods of defining the penalty stiffness.

4.2.2.2 Results and Discussion

The shear stress shown in the picture 4-24 and 4-25 is the residual shear stress after the rolling process is finished. Figure 4-24 presents typical stress edge effect on the free edge of the rolled plate by using the old method. And such high stress patch

disappears in the new method. The high shear stress at the right hand of the plate is caused by the initial force to get plate moving forward. Note that the high shear stress at the edge might cause the instability of the system. Since the plate is totally in the state of plastic deformation, such a non-equilibrium stress configuration will continue the plastic deformation and increase the unexpected plastic strain even after the rolling process is finished.

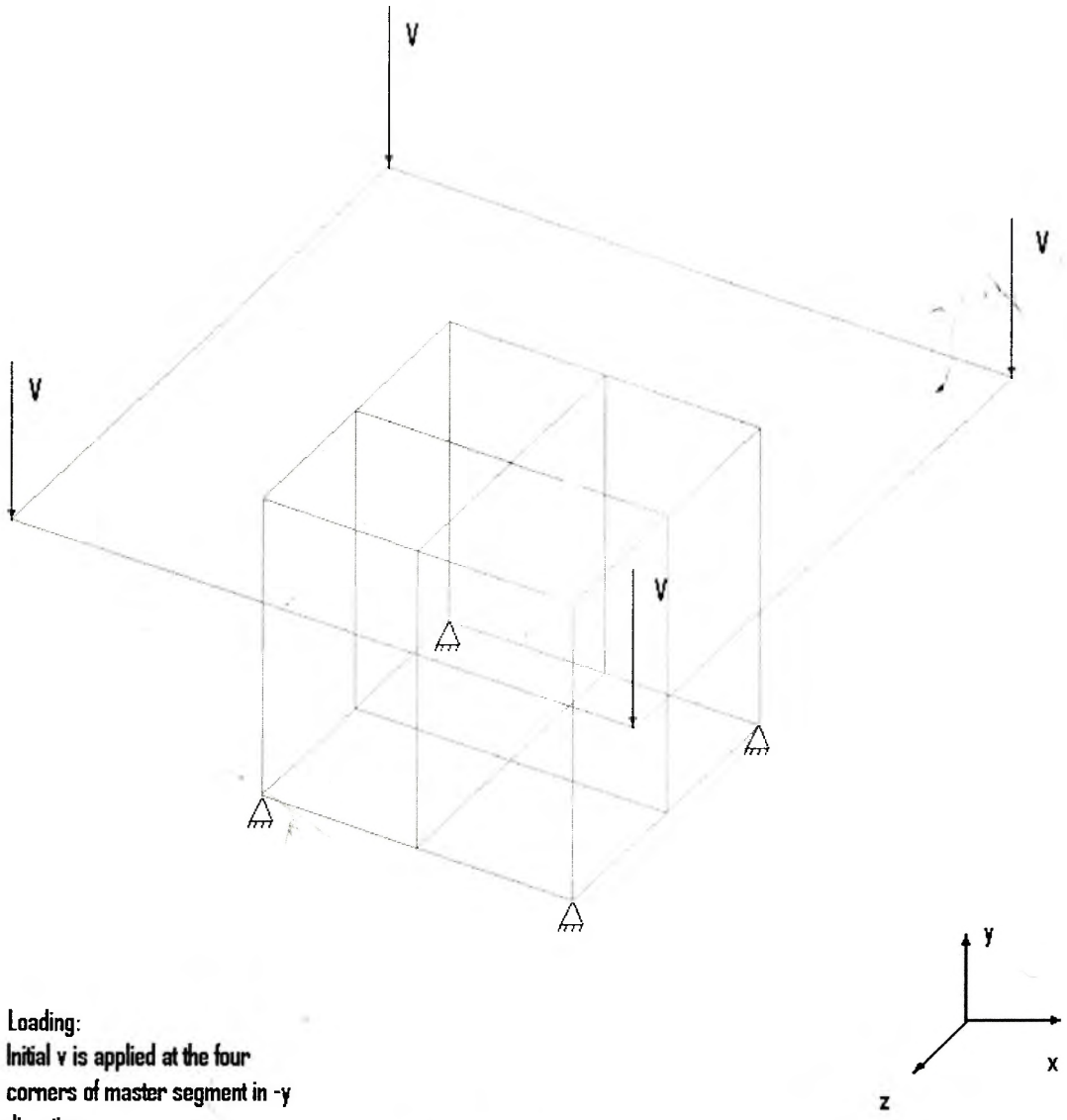

Fig. 4-1 Block Compression with Initial Velocity Loading

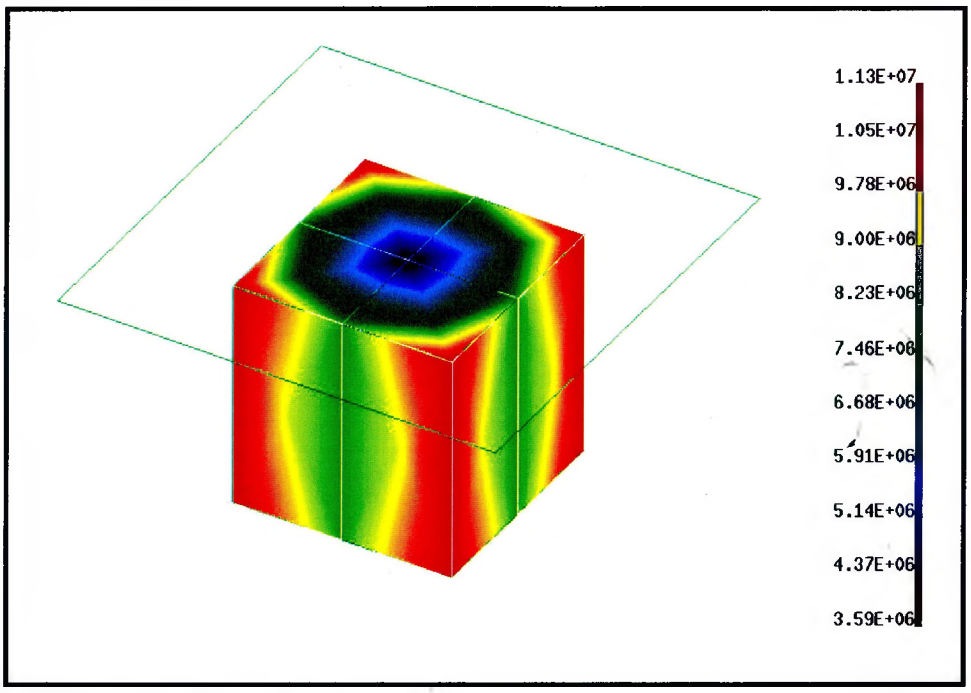

Fig. 4-2 Von Mises Stress (MPa) at the Time 0.007 (Old Method)

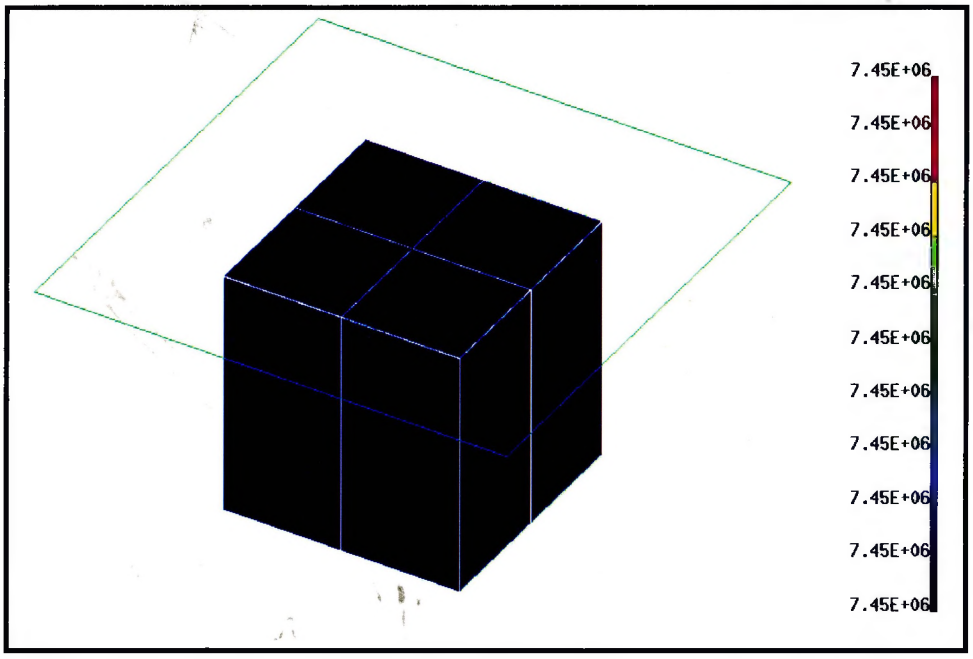

Fig. 4-3 Von Mises Stress (MPa) at the Time 0.007 (New Method)

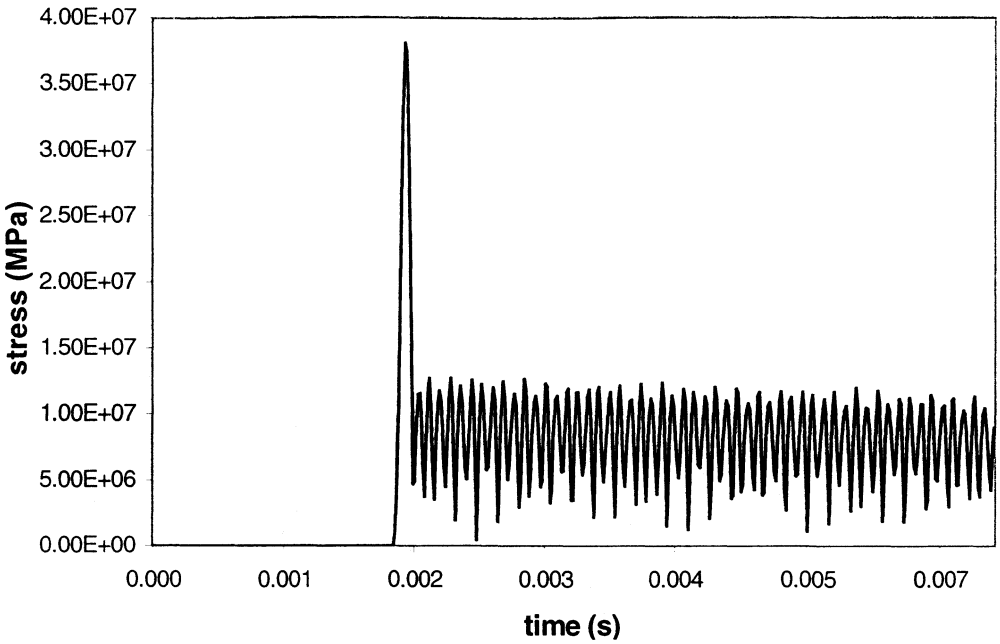

Fig. 4-4 Von Mises Stress during the Contact (Old Method)

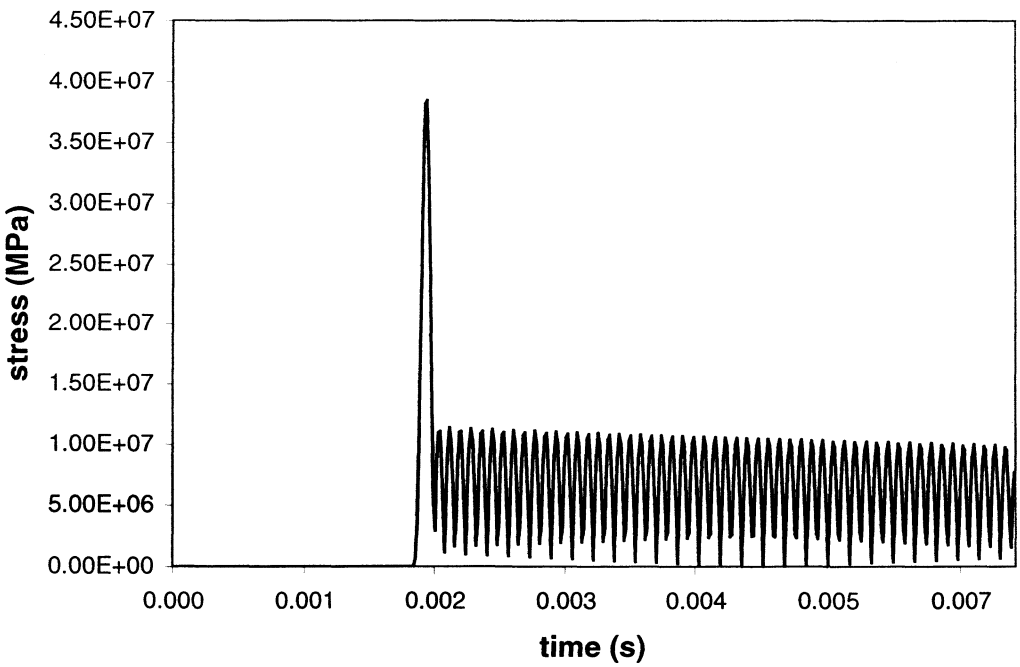

Fig. 4-5 Von Mises Stress during the Contact (New Method)

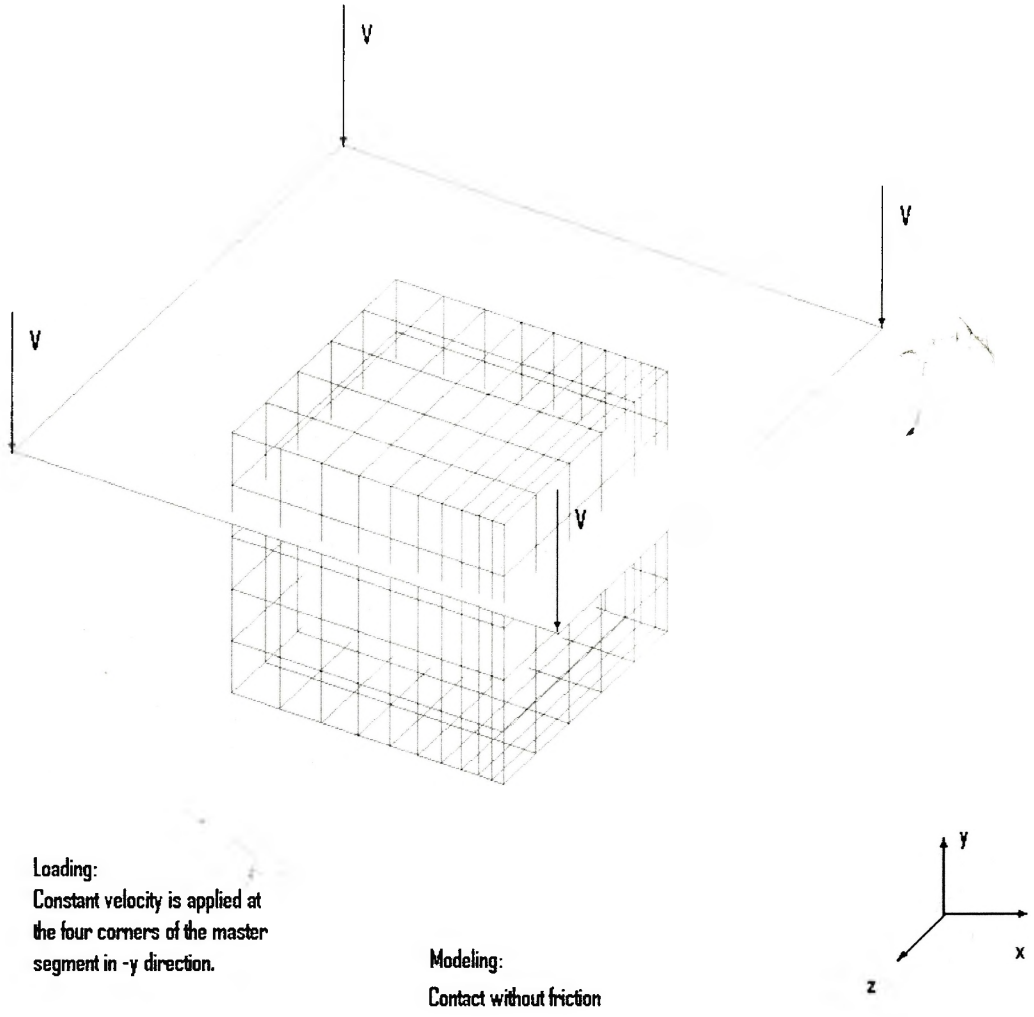

Fig. 4-6 Block Compression with Constant Velocity Loading Control

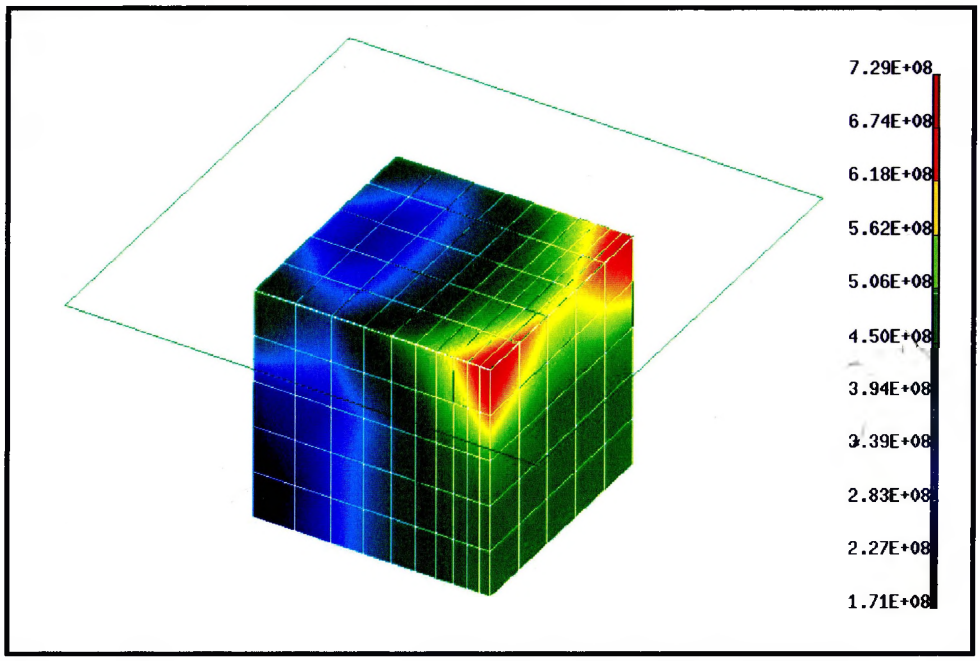

Fig. 4-7 Von Mises Stress (MPa) at the Time 0.007 (Old Method)

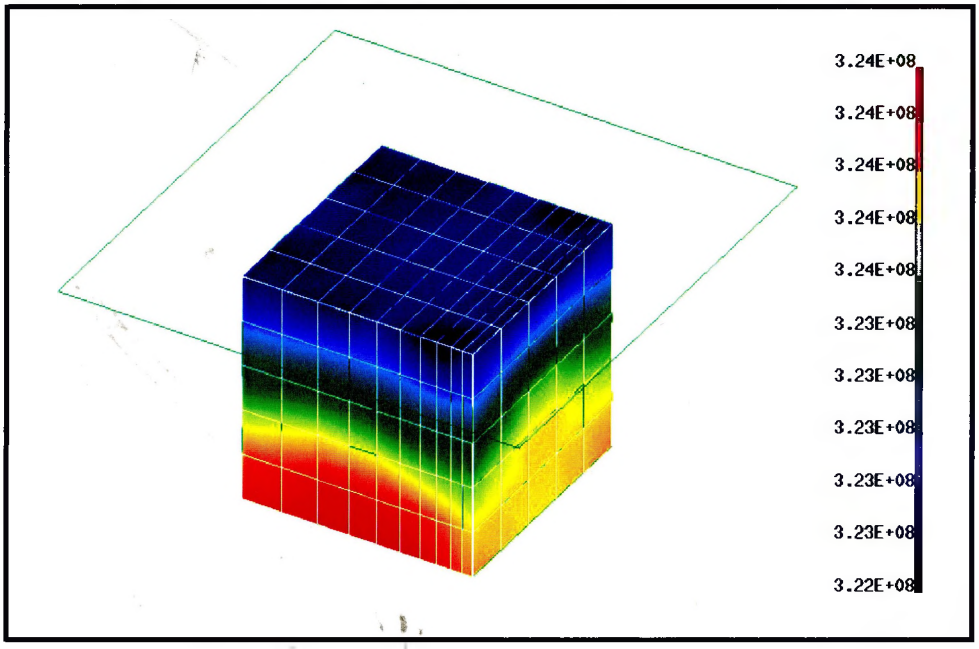

Fig. 4-8 Von Mises Stress (MPa) at the Time 0.007 (New Method)

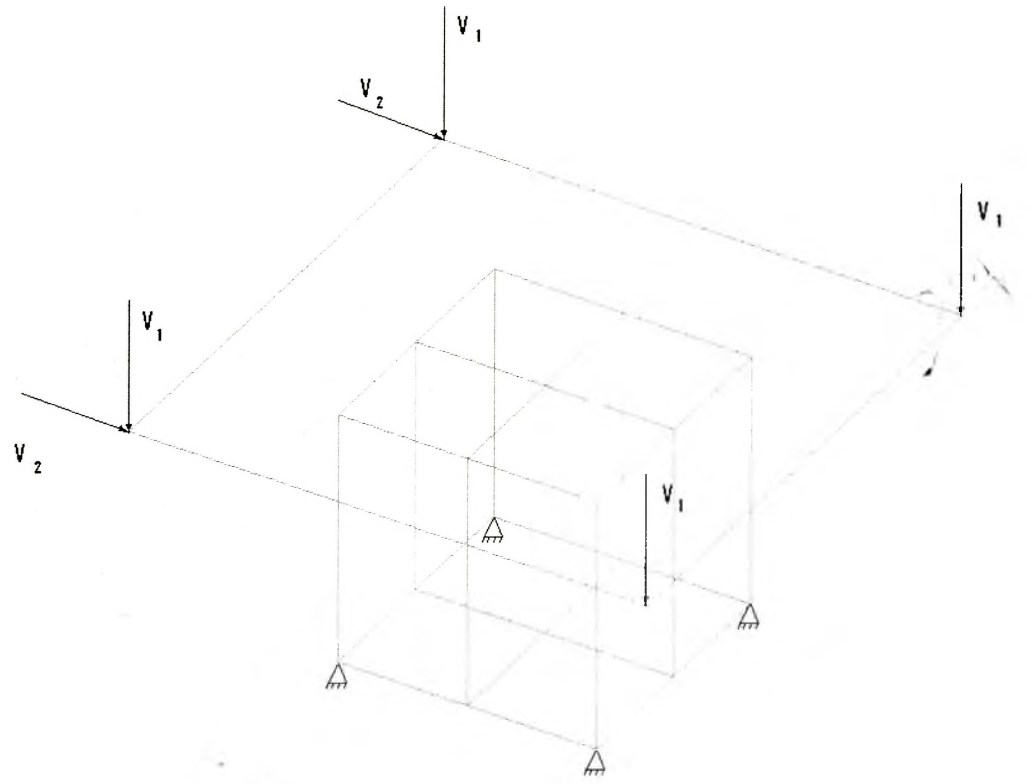

Loading:
1. Constant V1 is applied at the four corners of the master segment in -y direction during frist 0.003s, then keeps to zero
2. Constant V2 is applied at left two corners of the master segment in x direction after loading 1 is finished

Modeling:
1. Contact with friction
2. Periodic symmetry

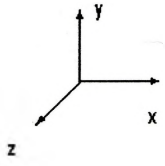

Fig. 4-9 Block Compression with Friction

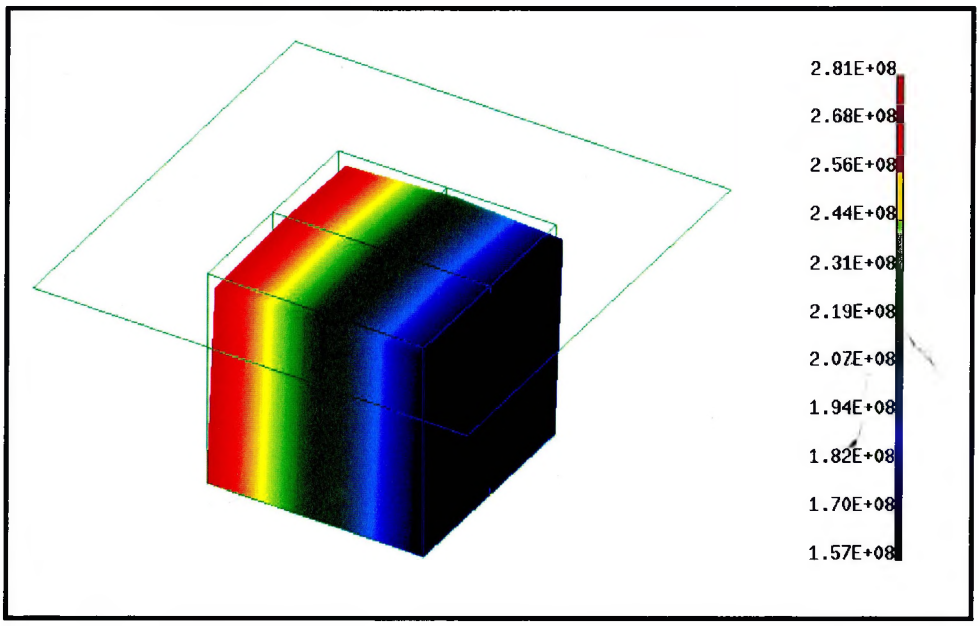

Fig. 4-10 Shear Stress (MPa) at the Time 0.007 (Old Method)

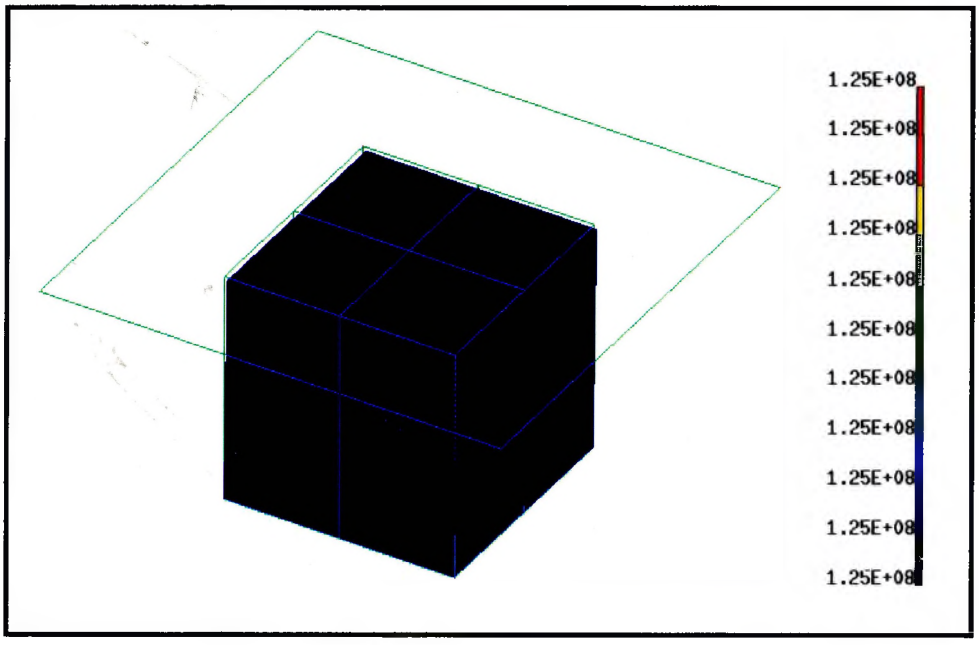

Fig. 4-11 Von Mises Stress (MPa) at the Time 0.007 (New Method)

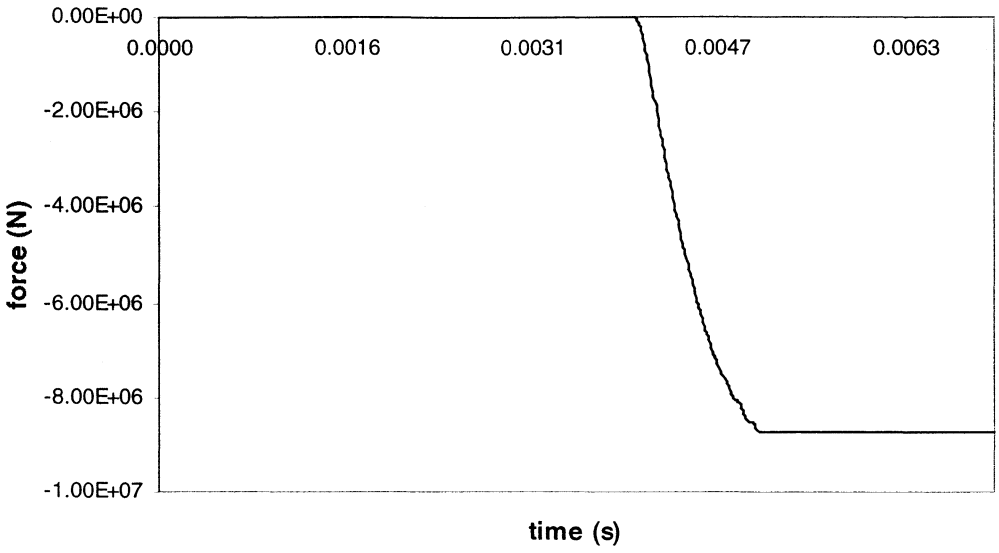

Fig.4-12 Contact Force in X Direction (Old Method)

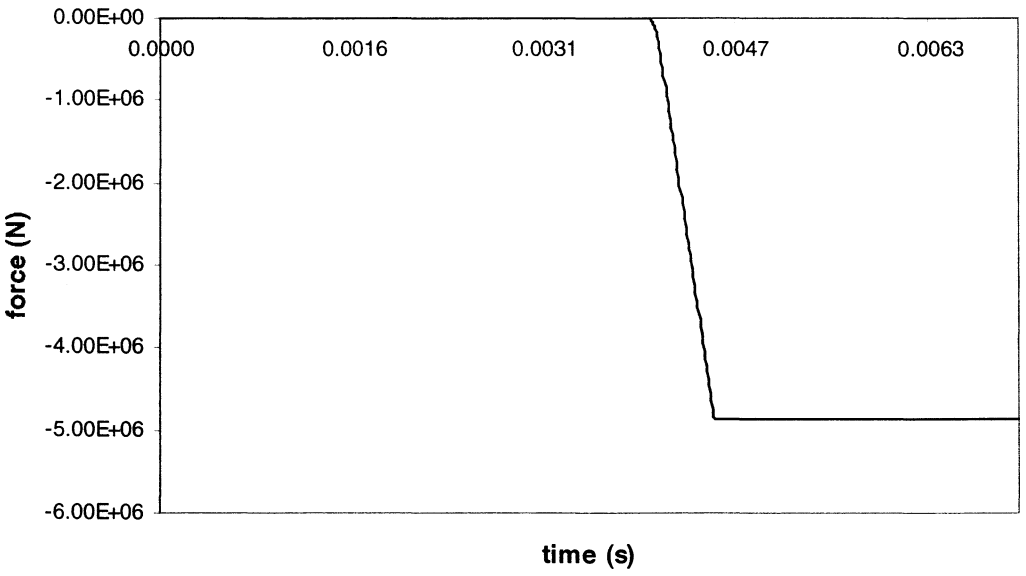

Fig.4-13 Contact Force in X Direction (New Method)

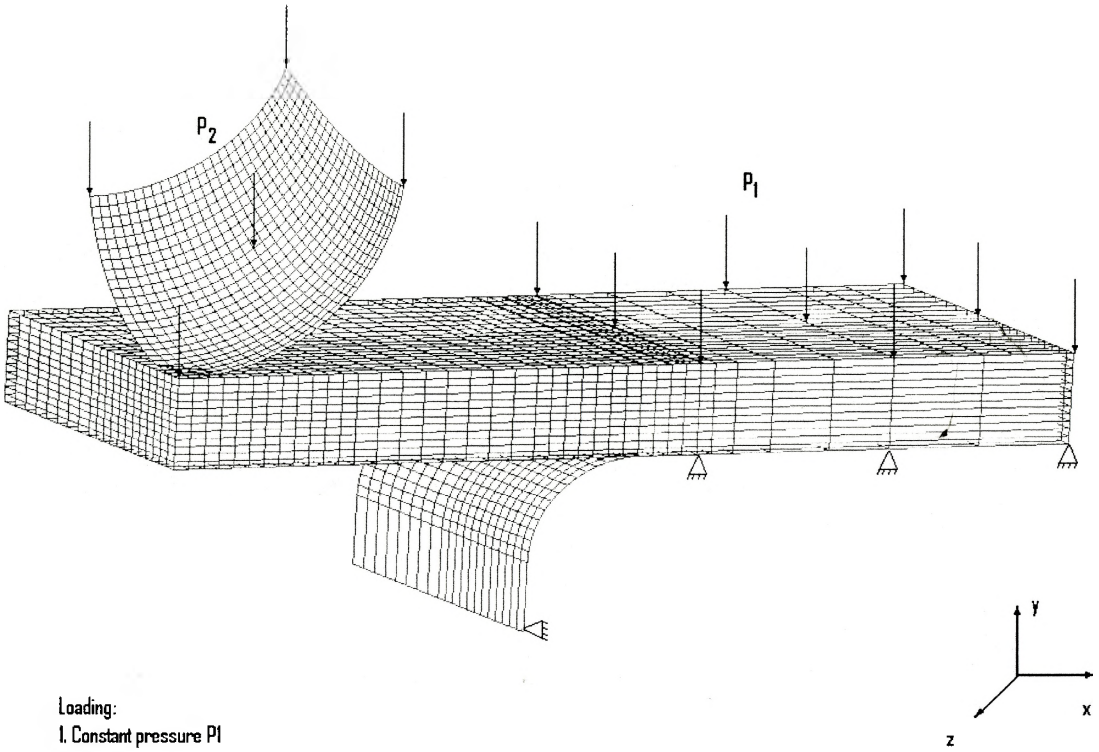

Fig.4-14 Finite Element Model of the Punch Test

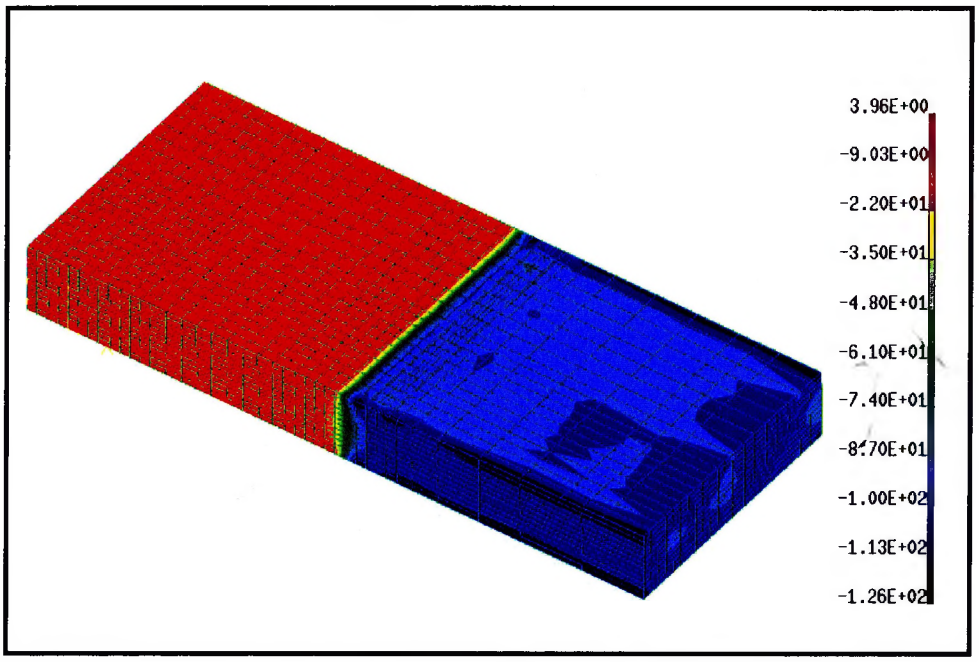

Fig. 4-15 Normal Stress (MPa) over the Clamped Section (Old Method)

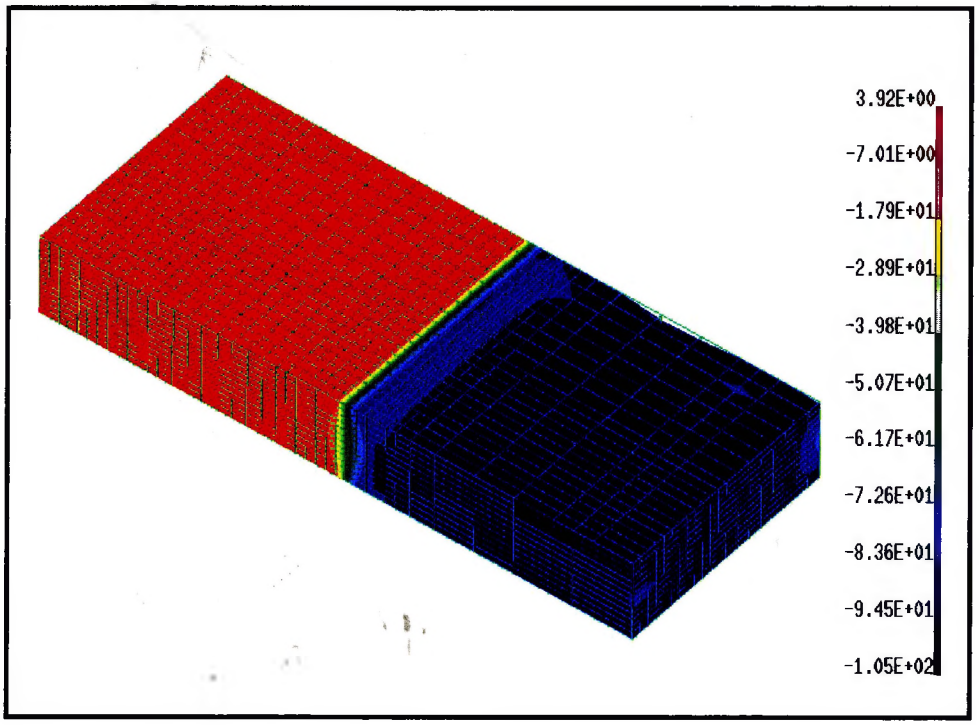

Fig. 4-16 Normal Stress (MPa) over the Clamped Section (New Method)

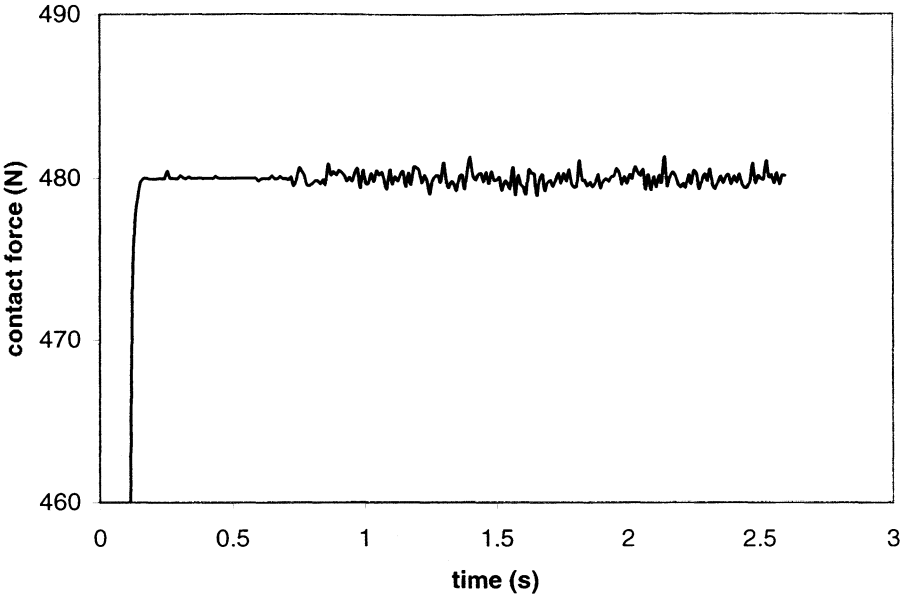

Fig. 4-17 Contact Force over the Clamped Section (Old Method)

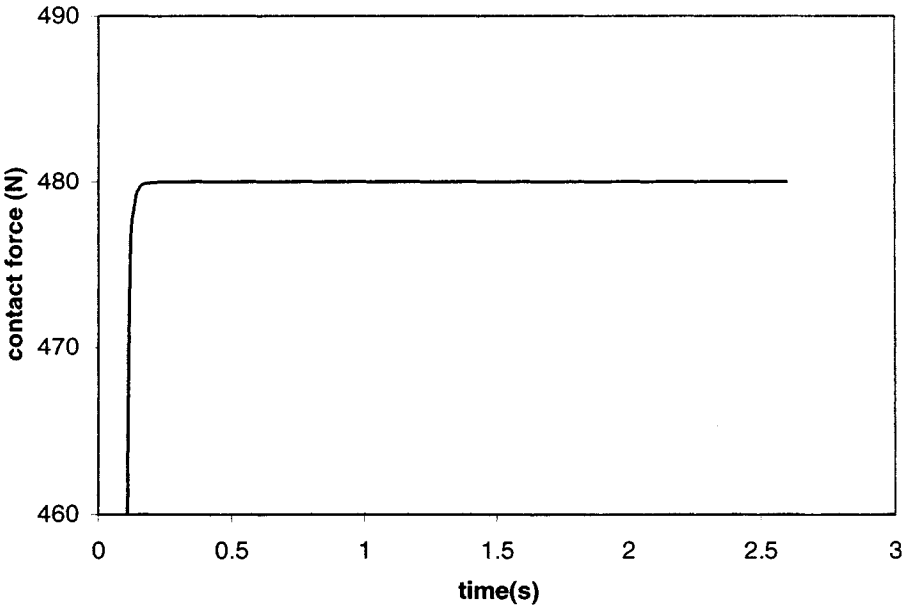

Fig. 4-18 Contact Force over the Clamped Section (New Method)

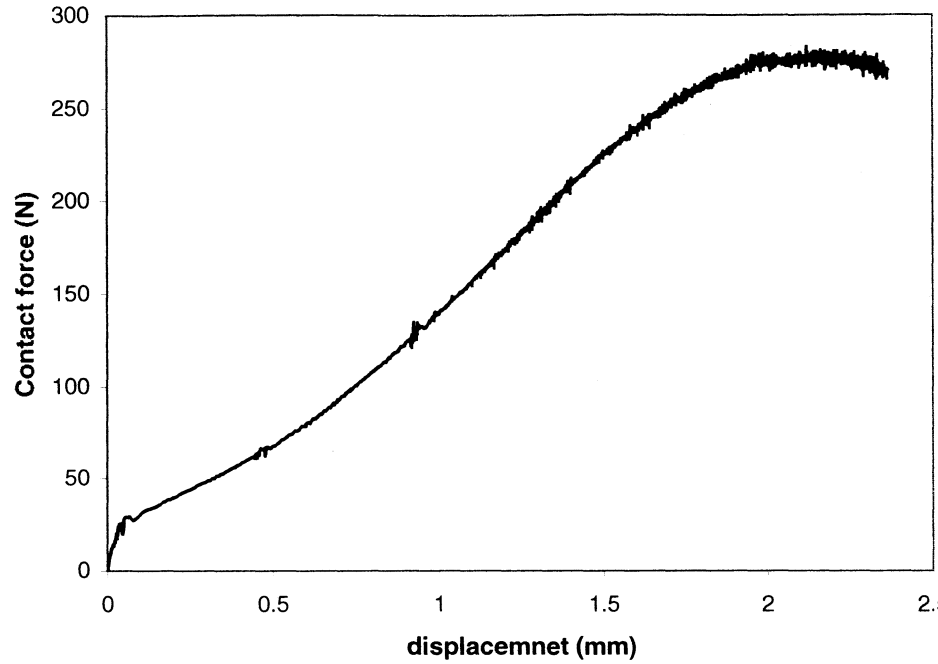

Fig. 4-19 Contact Force over Punched Section (Old Method)

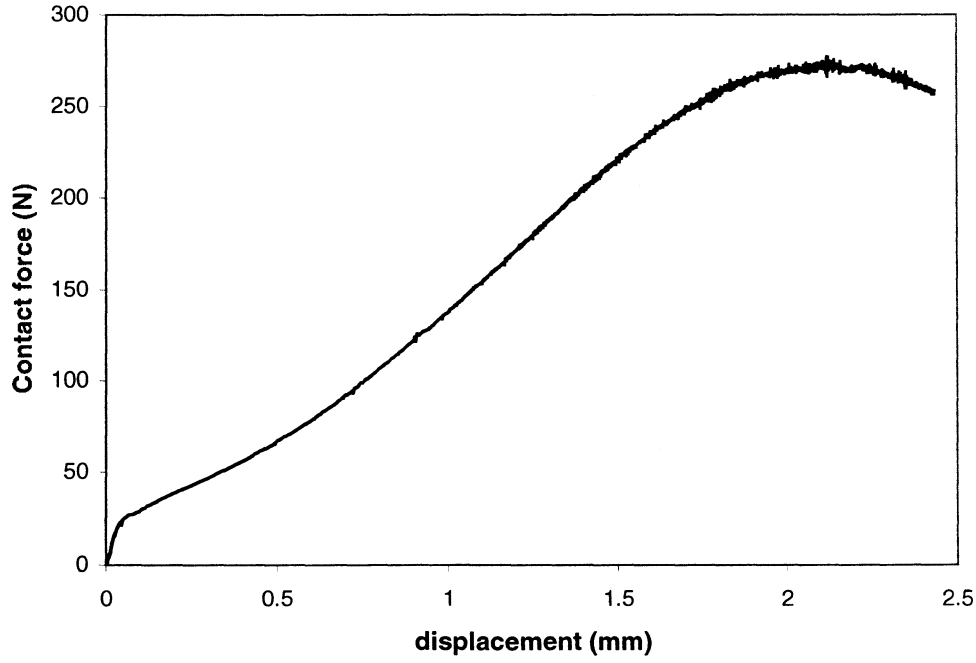

Fig. 4-20 Contact Force over Punched Section (New Method)

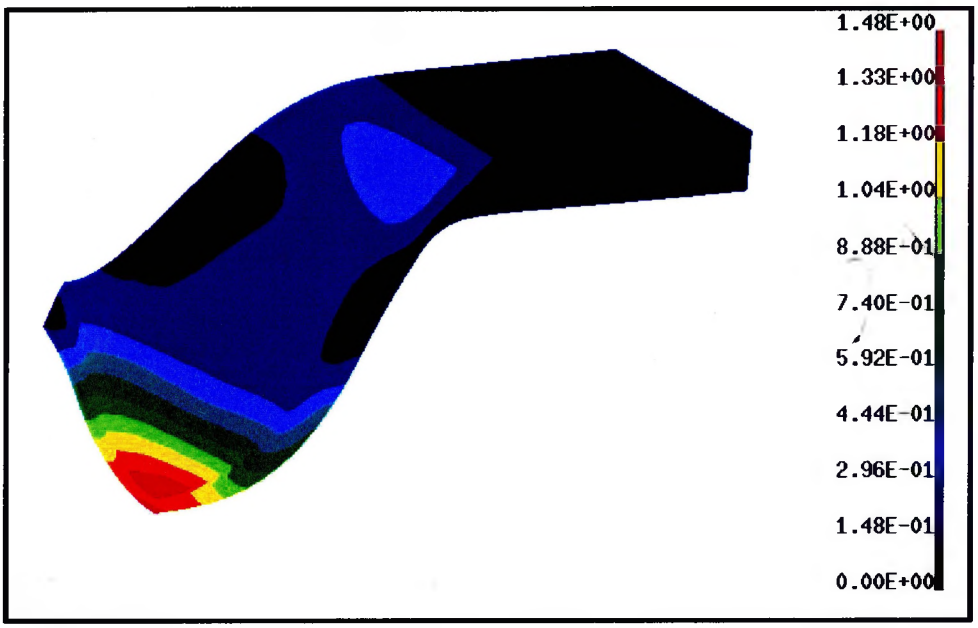

Fig. 4-21 Plastic Strain (mm) over Punched Section (Old Method)

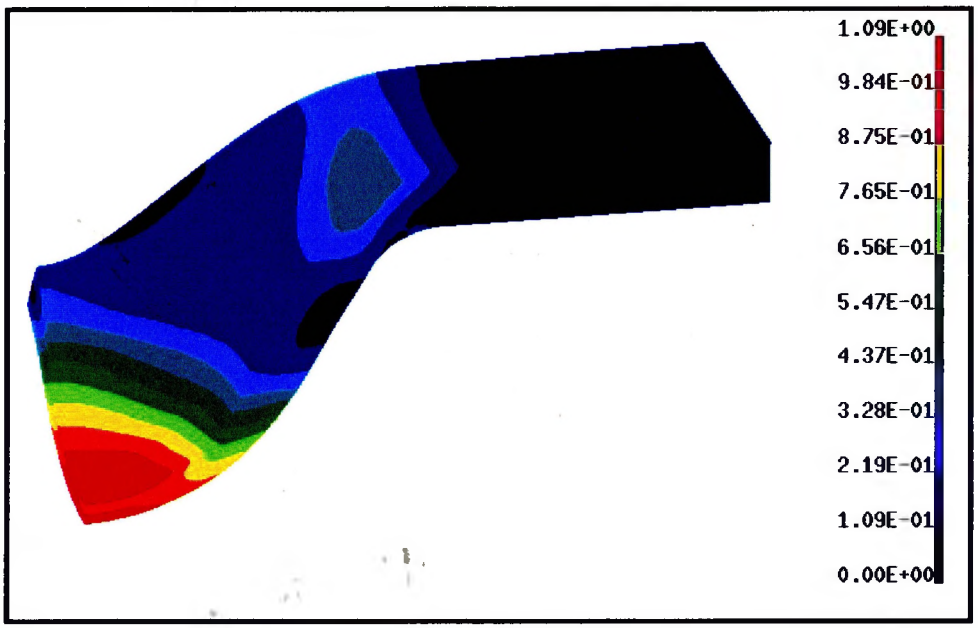

Fig. 4-22 Plastic Strain (mm) over Punched Section (New Method)

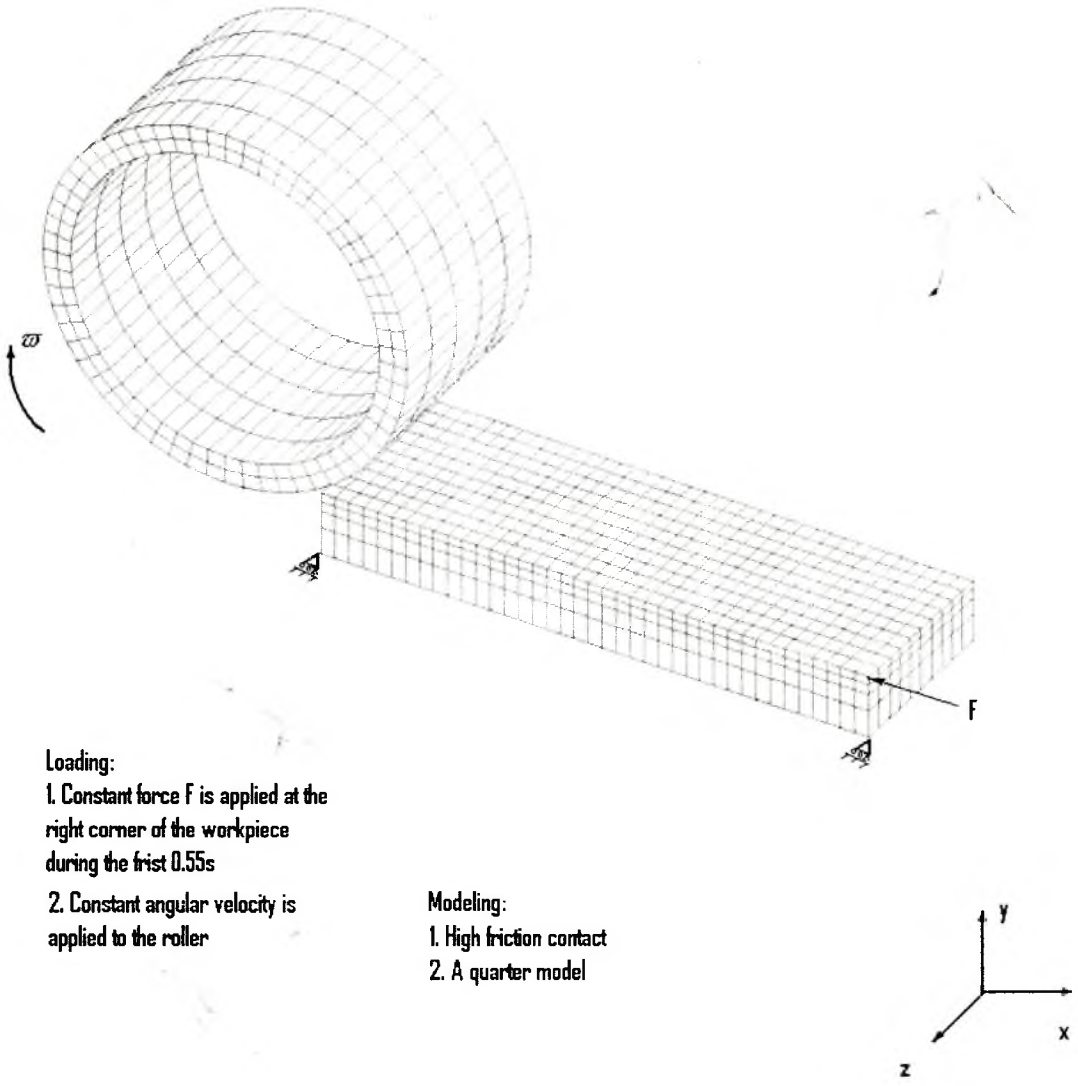

Fig. 4-23 Finite Element Model of Rolling Process

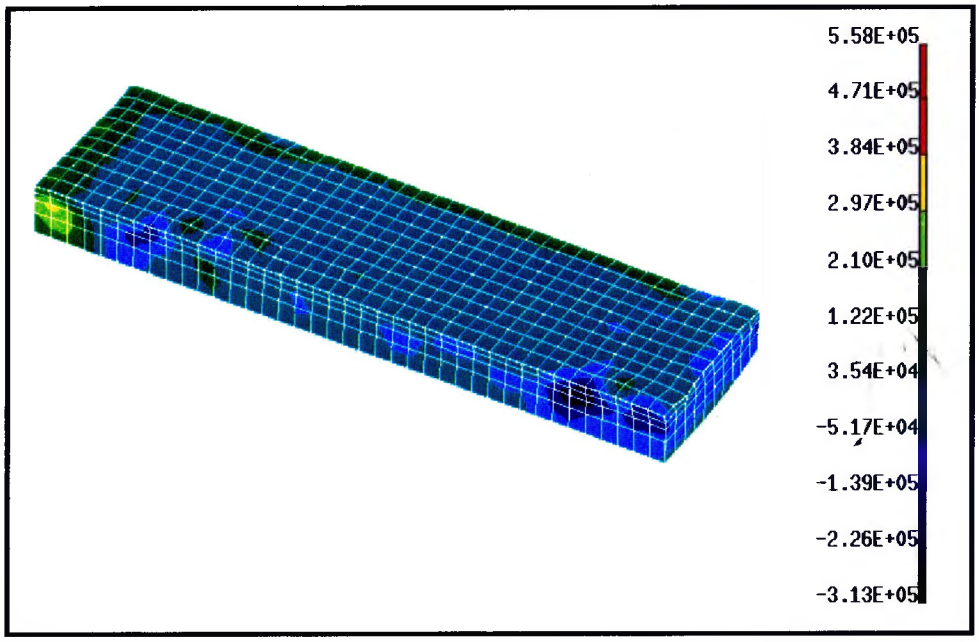

Fig. 4-24 Shear Stress (MPa) Distribution (Old Method)

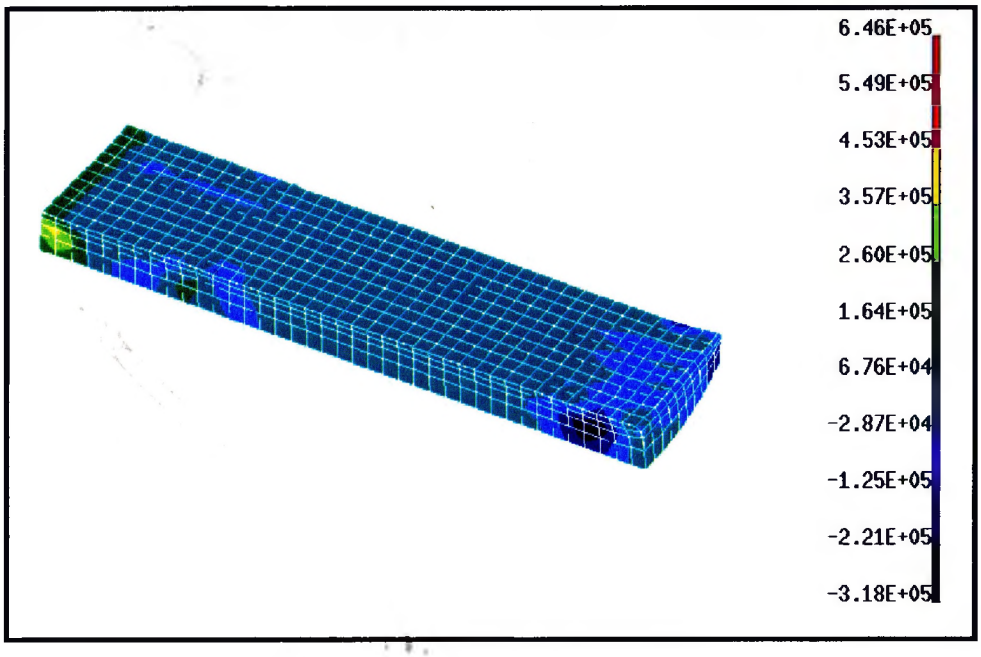

Fig. 4-25 Shear Stress (MPa) Distribution (New Method)

CHAPTER 5

CONCLUSIONS AND RECOMMENDATIONS

5.1 Conclusion Related to the New Method to Define the Penalty Stiffness

A new way to define the contact stiffness is developed and implemented with its application in several tests and cases. The new method ensures that the slave node forces are consistently related to contact pressure and shear stress through the appropriate slave surface geometry. This permits a uniform stress distribution on the contact surface without the concern for the presence of edges or mesh nonuniformity. Also the new method will avoid the numerical noise for the dynamic transient analysis in the contact problem by using the explicit method. The new penalty stiffness is obtained in terms of reference penetration and reference pressure which is defined by the user according to the condition of actual contact situation. Stability is no more difficult to ensure than the other methods, and the user inputs have a clear physical meaning. Also, the computational efficiency is not a big problem because the time of slave area calculation is much smaller than that of numerical integration in the explicit method.

5.2 Recommendations for the Reference Penetration and Pressure Selection

In the new method, since the penalty stiffness is defined by the user, the selection of both the reference penetration and pressure will greatly influence the simulation

performance. High pressure will cause a high contacting force and big reference penetration may cause excessive actual penetration. From comparison of the results of both methods, it is recommended that the reference contact pressure should correspond to the yield stress of a contacting material, and the reference penetration should be a fraction of the element depth below the contact. This can ensure that excessive penetration will not occur and at the same time it will keep the stability of system for the contact problem with the explicit method.

5.3 Recommendation for Future Work

With regard to finite element solution to the general contact problem in the penalty method, the selection of penalty stiffness is truly problem-dependent. Automatic penalty stiffness gives the users an easy way to implement the analysis but raises the problem of the stress edge effect. The new method provides an approach to eliminate such unexpected high stress, but users have to define the contact parameters according to the actual situations.

The case studies show that the user defined parameters, the reference penetration and reference pressure, may greatly influence the final results. A study of influence of varied control parameters with different modeling conditions would be of great help for industrial application and deep understanding of the mechanism of contact. Computational efficiency with the introduction of the slave area calculation is also worth study since in the explicit method time efficiency is always a big concern, especially for multi-body contact models with large numbers of degree of freedom.

REFERENCES

[1] P. Arthur, Boresi., "Advanced Mechanics of Materials", 4th Edition John Wiley&Son Inc.

[2] K. L. Johnson, "Contact Mechanics", Cambridge University Press, 1985.

[3] Z. H. Zhong, "Finite Element Procedure for Contact-Impact Problems", Oxford University Press, 1993.

[4] J. S. Strenkowski, J.T. Carroll, "A Finite Element Model of Orthogonal Metal Cutting, Journal of Engineering for Industry", Vol., 107, Nov., 1985.

[5] T. Obikawa, H. Sasahara, T. Shirakashi, E. Usui, "Application of Computational Machining Method to Discontinuous Chip Formation", Journal of Manufacturing Science and Engineering, Vol., 119/667, Nov., 1997.

[6] A. J. Shih, "Finite Element Simulation of Orthogonal Metal Cutting", Journal of Engineering for Industry, 84/Vol., 117, Feb., 1995.

[7] J. M. Huang, A, J. Black, "An Evaluation of Chip Separation Criteria for the FEM simulation of Machining", Journal of Manufacturing Science and Engineering, Vol., 118/545, Nov., 1996.

[8] J. J. Park, "Application of Three Dimensional Finite Element Analysis to Shape Rolling Processes", Journal of Engineering for Industry, 36/Vol., 112, Feb., 1990.

[9] V. Bhargava, "An Elastic-Plastic Finite Element Model for Rolling Contact", Journal of Applied Mechanics, 67/Vol., 52, 1985.

[10] Kulkarni, Elastoplastic, "Finite Element Analysis of Three Dimensional Pure Rolling Contact at the Shakedown Limit", Journal of Applied Mechanics, 57/Vol., 57, 1990.

[11] W. Q. Cheng, "Computational Finite Element Analysis and Optimal Design for Multibody Contact System", Computer Methods in Applied Mech. Eng., 31/Vol., 71, 1988.

[12] Torstenfelt, "Contact Problems with Friction in General Purpose Finite Element Computer Programs". Computers and Structures, 487/ Vol., 16, 1983.

[13] Okamoto, "Finite Element Incremental Contact Analysis with Various Frictional Conditions", Int. J. Num. Meth. Eng., 337/ Vol., 14, 1979.

[14] H. A. Francis, "A Finite Element Model for Two Concentric Nearly Circular Rings in Partial Contact", Computers and Structures, 169/ Vol., 17, 1983.

[15] R. D. Cook, "Concept and Application of Finite Element Analysis", 3rd edition John Wiley&Sons, 1989.

[16] K, J. Bathe, "Finite Element Procedure", Prentice Hall, 1996

[17] K. J. Bathe, "On Finite Element Analysis of Large Deformation Frictional Contact Problems", Unification of Finite Element Methodds, Elsevier Science Publishers, B.V. 123, 1984.

[18] M. G. Katona, "A Simple Contact-Friction Interface Element with Application to Bureid Culverts", Int. J. for Num. And Anal. Meth. In Geom., 371, Vol., 7, 1984.

[19] N. Chandrasekaran, W.E. Haisler, R.E. Goforth, "A Finite Element Solution Method for Contact Problems with Friction", International Journal for Numerical Methods in Engineering, Vol., 24, 477-495.

[20] Seung Jo Kim, Jin Hee Kim, "Finite Element Analysis of Laminated Composites with Contact Constraint by Extended Interior Penalty Method", International Journal for Numerical Methods in Engineering, Vol., 36, 3421-3439.

[21] O. C. Zienkiewicz, "The Finite Element Method", 3rd edition, McGraw-Hill, London, 1997.

[22] N. Kikuchi, Y. J. Song, "A Smoothing Technique for Reduced Integration Penalty Methods in Contact Problem", Int. J. Num. Meth. Engng., 18, 343-350, 1982.

[23] N. Chandrasekaran, W. E. Haisler and R.E.Goforth, "A Finite Element Solution Method for Contact Problem with Friction", Int. J. Num. Meth. Engng., 24, 477-495, 1987.

[24] R. F. Kulak, "Adaptive Contact Elements for Three-dimensional Explicit Transient Analysis", Comput. Meths. Appl. Mech. Engng., 72, 125-151, 1989.

[25] J. O. Hallquist, "LS-DYNA Theoretical Manual", Livermore Software Technology Corporation, 1998.

[26] ABAQUS Explicit Users, Volume II, Version 6.1, 2000.

[27] R. G. Sauve, "A Contact-impact Algorithm for Three-dimensional Finite Deformation", Ontario Hydro Research Division Report, No., 90-314-K, 1990.

[28] J. O. Hallquist, "A Numerical Treatment of Sliding Interfaces and Impact", Report of Lawrence Livermore Laboratory.

[29] Samuel W. Key, "A Data Structure for Three-Dimensional Sliding Interfaces", Internal Conference on Computational Mechanics, May 25-29, Tokyo, Japan.

[30] J. M. Manuel, Barata Marques, Paulo A. F. Martins, "Three-Dimensional Finite Element Contact Algorithm for Metal Forming", International Journal for Numerical Methods in Engineering, Vol., 30, 1341-1354, 1990.

[31] Ted Belytschko, Mark O. Neal, "Contact-Impact by the Pinball Algorithm with Penalty and Lagrangian Methods", International Journal for Numerical Methods in Engineering, Vol., 31, 547-572, 1991.

[32] Jerry I. Lin, Ted Belytschko, "A Three-Dimensional Impact-Penetration Algorithm with Erosion", Computers and Structures, Vol., 25, No., 1, 95-104, 1987.

[33] O. C. Zienkiewicz, "A Note on Numerical Computation of Elastic Contact Problems", Int. J. Meth. Eng., 913/Vol., 9, 1975.

[34] Gu, "Moving Finite Element Analysis for the Elastic Beam in Contact Problem", Computer and Structures, 571/Vol., 1986.

[35] Heber, "A Mixed Eulerian-lagrangian Displacement Model for Large Deformation Analysis in Solid Mechanics", Comp. Meth. Appl. Mech. Eng., 277/Vol., 43, 1984.

[36] N. Patir and H.S. Cheng, "Application of Average Flow Model to Lubrication between Rough Sliding Surfaces", ASME, J, Lubri. Tech., 101, 220-230,1979.

[37] D. C. Sun, K. K. Chen and H. D. Nine, "Hydrodynamic Lubrication in Hemispherical Punch Stretch Forming—Modified Theory and Experimental Validation", Int. J. Mech. Sci., 29, 761-776, 1987.

[38] W. R. D. Wilson, "Friction and Lubrication in Bulk Metal-Forming Process", J. Appl. Metal Working, 1-19, 1979.

[39] W. K. Liu, Yu-Kan Hu, Ted Belytschko, "ALE Finite Elements with Hydrodynamic Lubrication for Metal Forming", Nuclear Engineering and Design, 138, 1-10, 1992.

[40] B. Fredriksson, "Numerical Solution to Contact Friction and Crack Problems with Applications", Eng, comp., 133/Vol., 1, 1984.

[41] L. E. Malvern, "Introduction to the Mechanics of a Continuous Medium", Prentice Hall.

[42] W. F. Chen, "Plasticity for Structural Engineers", New York, Springer-Verlag, c1998.

[43] W. K. Liu, S. J. Ong, R. A. Uras, "Finite Element Stabilization Matrices - a Unification Approach", Computer Methods in Applied Mechanics, Vol., 53, 13-46, 1985.

[44] W. F. Hosford and R.M. Caddell, "Metal Forming—Mechanics and Metallurgy", Prentice-Hall, 1983, USA.

[45] O. J. Hallquist, "A Numerical Treatment of Sliding Interfaces and Impact", Int. Computational Techniques for Interface Problems, K.C. Park and D.K. Gartling (eds.), AMD Vol., 30, ASME New York, 1978.

[46] R. G. Sauvé, "H3DMAP Version 6.0 - A General Three-Dimensional Finite Element Computer Code for Linear and Nonlinear Analysis of Structures", Ontario Power Technologies Report No. A-NSG-96-120, Rev. 1, 1999.

[47] W. K. Lee, D. R. Metzger, A. Donne, O. E. Lepik,"The Use of a Small Punch Test Procedure to Determine Mechanical Properties", Small Specimen Test Techniques, ASTM STP 1329, W.R. Corwin, S.T. Rosinski, and E. van Walle, Eds., American Society for Testing and Materials, 1997.